TÜBİTAK

Turkish Journal of Earth Sciences

http://journals.tubitak.gov.tr/earth/

Research Article

Turkish J Earth Sci
(2019) 28: 479-499

doi:10.3906/yer-1902-35

Late Quaternary landscape evolution of the southern Marmara region: paleogeographic implications for settlements, NW Turkey

Nizamettin KAZANCI[1,2], Zeynep ERGUN[1,*], Kaan İREN[3], Suzanne A.G. LEROY[4], Sonay BOYRAZ ARSLAN[2,5], Salim ÖNCEL[6], Koray KOÇ[1,7], Alper GÜRBÜZ[8]

[1]Department of Geological Engineering, Faculty of Engineering, Ankara University, Gölbaşı, Ankara, Turkey
[2]Turkish Association for Conservation of Geological Heritage (JEMİRKO), Anıttepe, Ankara, Turkey
[3]Archaeological and Archaeometric Research and Application Centre of Sıtkı Koçman University, Muğla, Turkey
[4]Aix Marseille University, CNRS, Minist Culture, LAMPEA, UMR 7269, Aix-en-Provence, France
[5]Department of Mining Analyses and Technologies, General Directorate of Mineral Research and Exploration (MTA), Ankara, Turkey
[6]Department of Environmental Engineering, Faculty of Engineering, Gebze Technical University, Çayırova, Gebze, Kocaeli, Turkey
[7]Department of Geological Engineering, Faculty of Engineering, Akdeniz University, Antalya, Turkey
[8]Department of Geological Engineering, Faculty of Engineering, Niğde Ömer Halisdemir University, Niğde, Turkey

Received: 23.02.2019 • **Accepted/Published Online:** 27.05.2019 • **Final Version:** 22.07.2019

Abstract: This study presents the late Quaternary evolution of the southern Marmara region in northwestern Turkey and discusses the suitability of the area for settlements. It is based on interpretation of sediment analyses together with radiometric dates obtained from drilling cores. As three-fourths of the southern Marmara region (ca. 30,000 km^2) is covered by the Susurluk Drainage Basin (SDB), the study focuses on this basin. The SDB has a concave surface morphology dipping northward, with highlands in the south (ca. 1300–1700 m a.s.l.) and lowlands in the north (ca. 0–250 a.s.l.). Lake Manyas, Lake Ulubat, and south-north flowing rivers, together with deep gorges and large valleys, are basic elements of the landscape. Quaternary deposits are largely confined to the late Pleistocene and Holocene time interval. Results suggest that, as a whole, the Southern Marmara region has been subjected to intense erosion up to the Late Pleistocene. During the Late Pleistocene and Holocene, depositional dynamics and channel migrations are recorded in river valleys, where sediments evidence occurrences of flooding and backswamps. Landscape analyses show that the SDB was not attractive for human settlements in the Late Holocene, with the exception of the Daskyleion and Appolonia sites, in opposition to other parts of western Anatolia, which have been densely occupied since the Chalcolithic Age. According to our results, the location of Daskyleion on a hill near Lake Manyas was likely chosen for security reasons. Lake water and large permanently wet areas (swamps) may have indeed provided a natural contribution to the defense of this Phrygian town.

Key words: Quaternary, Lake Manyas, Daskyleion, Marmara region, Holocene, Antic settlements

1. Introduction

Northwest Turkey comprises two straits (the Çanakkale-Dardanelles strait and İstanbul-Bosphorus strait) and an inland sea (Sea of Marmara), which form the geographical boundary between Asia and Europe (Figure 1). The area delimited west, south, and east by the cities of Bursa, Kütahya, and Çanakkale, respectively, is known as the southern Marmara region in local descriptions. The morphology of the region is highly irregular due to a combination of active tectonics and different lithologies showing a variety of resistance to erosion (Ardel, 1960; Erol, 1981; Kazancı et al., 2014). Except for some north-south trending features, east-west and northeast-southwest trending depressions and elongated hills dominate the relief of the area (Erol, 1991). Lithological units mainly consist of Mesozoic and Cenozoic and to a lesser extent Paleozoic rocks. Quaternary units are limited and are associated with tectonic lines (Erol, 1981, 1982; Şaroğlu et al., 1987; Emre et al., 1998) (Figure 2). Relatively significant Pleistocene continental deposits are found in the lower Susurluk Drainage Basin (SDB), close to the Sea of Marmara (Figures 1 and 2). Varying landscapes of northwestern Anatolia and patchy distributions of Quaternary units have been known since the early 20th century from descriptions by many authors (i.e. Philippson, 1915; Chaput, 1936; Erentöz, 1956; Vita-Finzi, 1969). However, the stratigraphy and sedimentary facies of these deposits have not been described in this region.

* Correspondence: zergun@ankara.edu.tr

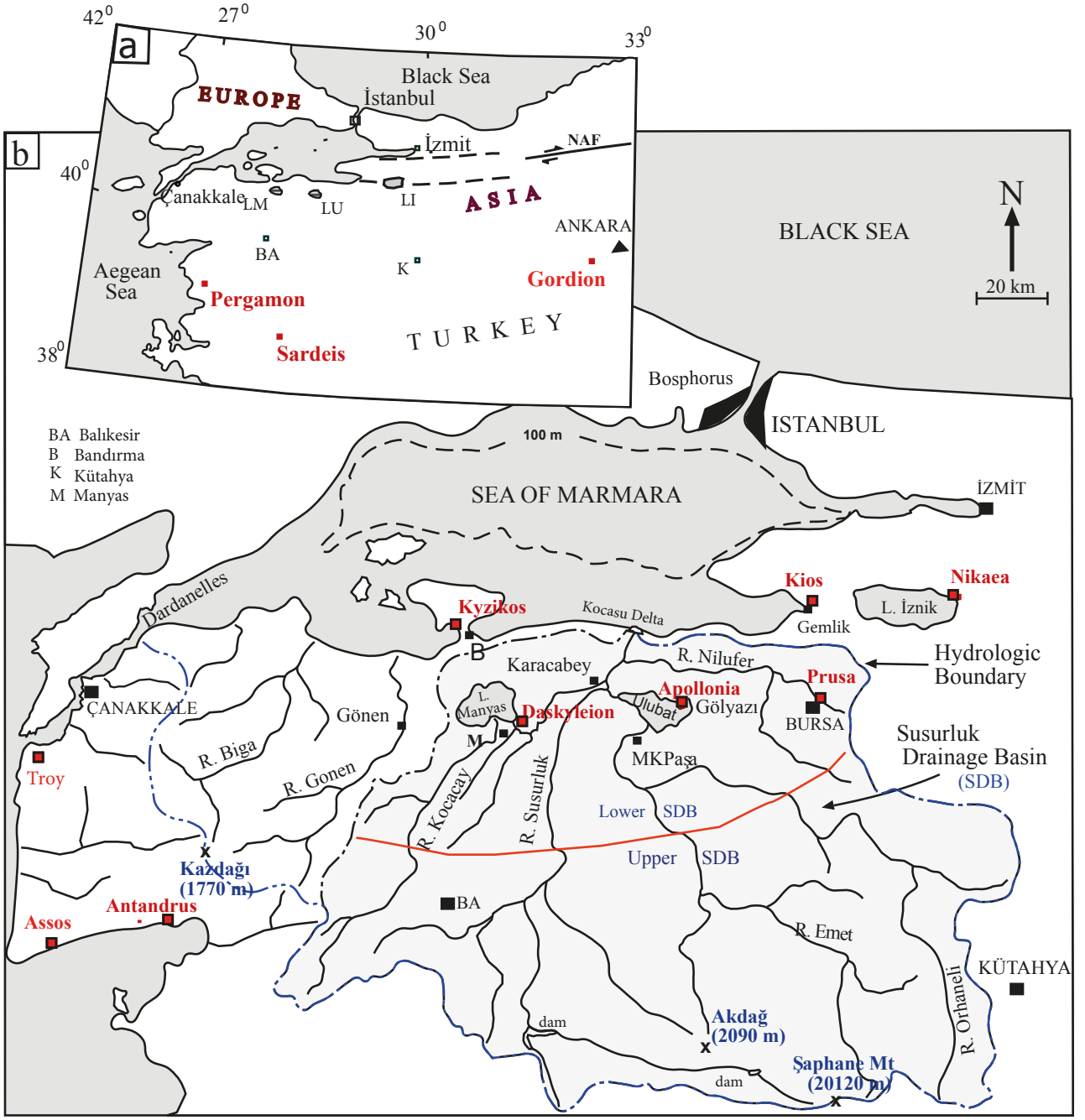

Figure 1. Site location. a) Location of southern Marmara lakes and some historical settlements. Note that the Dardanelle and Bosphorus straits separate the Asian and European continents. NAF = North Anatolian Fault, BA= Balıkesir, K = Kütahya, LM = Lake Manyas, LU = Lake Ulubat, LI = Lake İznik. b) The boundary and main streams of the Susurluk Drainage Basin. SDB = Susurluk Drainage Basin, R = rivers, MKPasa= Mustafakemalpaşa. Şaphane Mountain is on the hydrologic boundary. The highest peak, Akdağ, is located within the basin itself. In red are significant Iron Age settlements, most of which are close to the seas and straits.

Accordingly, the evolution of Quaternary landforms in the region has remained interpretative until now. One significant issue addressed by previous authors concerns the reconstruction of the evolution of the relationships of the southern Marmara lakes with the Sea of Marmara. Some studies argued for marine connections between the lakes and the seas (i.e. Ardel, 1954; Ardel and İnandık, 1957; Erinç, 1957; Meriç et al., 2007; Nazik et al., 2011), a reconstruction that other authors disagreed with (Emre et al., 1997, 1998; Yaltırak et al., 2011). The present study

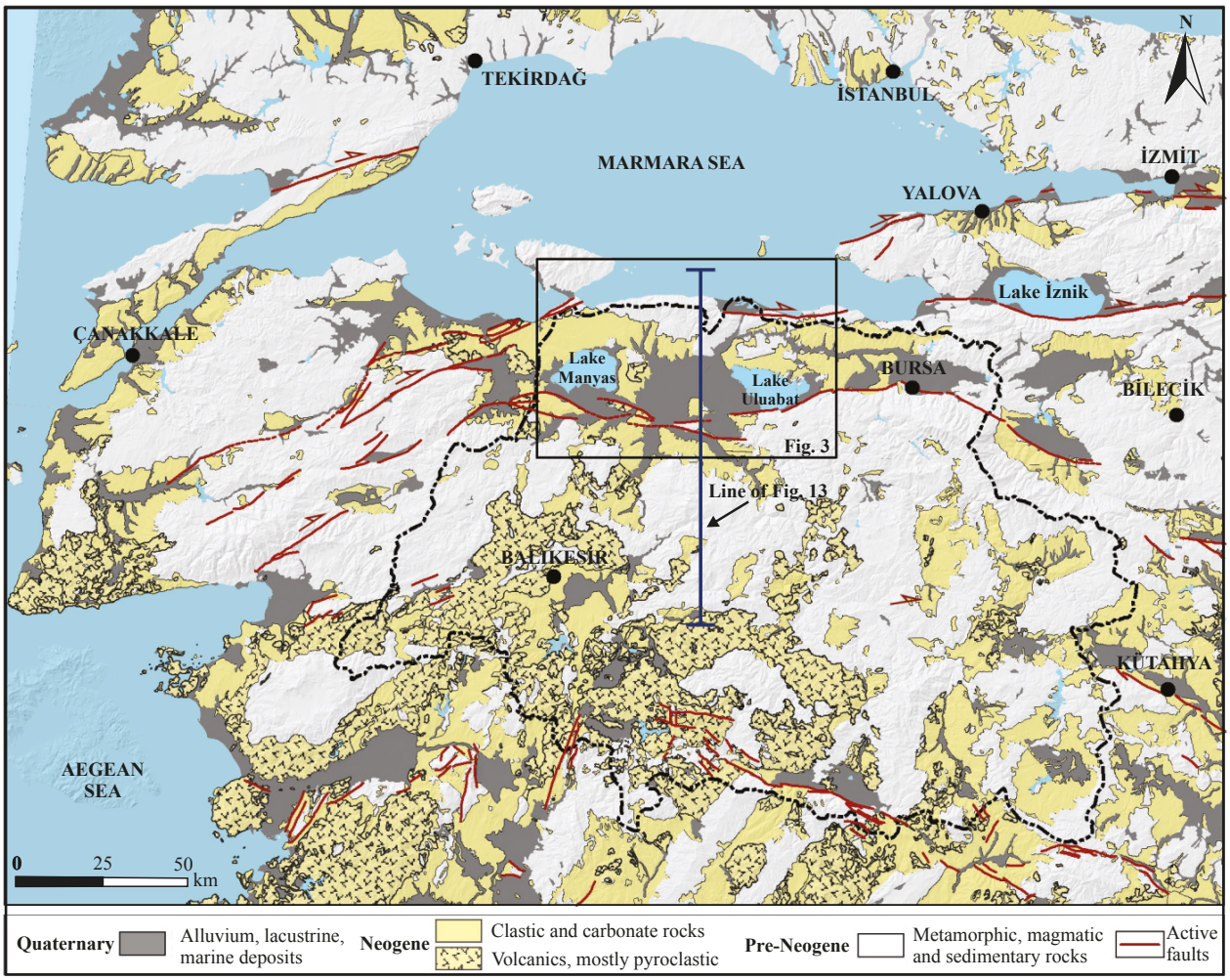

Figure 2. Main lithologies in the southern Marmara and northwestern Anatolia regions of Turkey, simplified from the MTA (2002). Active faults are from Şaroğlu et al. (1987). Note that Lakes Ulubat and Manyas are confined by the E-W trending faults that created the Ulubat-Manyas E-W elongated depression that parallels the southern shores of the Marmara Sea. SDB is shown by black dashed line. Sites of Figures 3 and 13 are also shown.

examines the Quaternary units from sediment cores in order to provide reliable data to shed light on this problem, and in particular to explain the development of Lakes Ulubat and Manyas and hence contribute to our understanding of the Late Quaternary landscape evolution of the Marmara region.

The second purpose of this study is to discuss the role of lithology, especially that of fine-grained and soft deposits, on land use and settlements in the southern Marmara region. Northwest Turkey, and particularly the Marmara region, including İstanbul, İzmit, and Bursa, is the most populated part of the country as it has a large potential for industry and agriculture because of land availability and freshwater availability from rivers and regulated lakes such as İznik, Manyas, and Ulubat (Figures 1–4). Recently population increase has been so high that the average number of inhabitants per km^2 is at least three times that of the whole country (TÜİK, 2016). In this region, a mild continental climate with four seasons (Figure 4) seems to be favorable for human settlements. In fact, the region has been attractive for settlement since the Bronze age, particularly in the Byzantine and Ottoman periods, as northwestern Anatolia is adjacent to the Mediterranean Sea and to Europe (Evliya Çelebi, 1648; Turney and Brown, 2007), as well as on the route to the Pontic (Euxinian) lands. The Çanakkale (Dardanelles) and İstanbul (Bosphorus) straits have been important factors favorable to migrations of animals and humans between Asia and Europe not only at present but also from the Early/Middle Pleistocene (Leroy et al., 2011; Özbek, 2012). Also, due to the importance of trade routes and economic wealth, important civilizations and ancient cities (i.e. Troy,

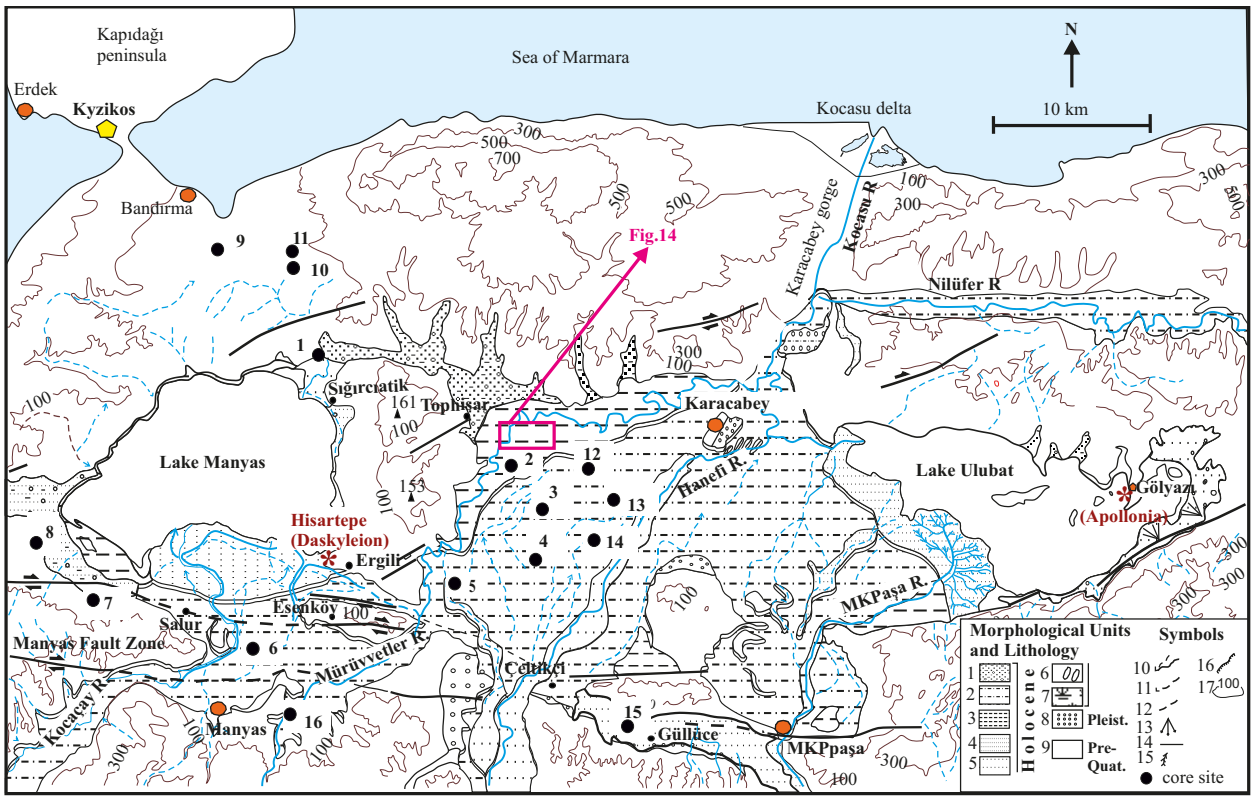

Figure 3. Geological and geomorphological map of the Manyas-Ulubat area. 1- Undifferentiated alluvium, 2- floodplain, 3- meandering channel and backswamp, 4- modern stream channel, 5- delta, 6- crevasse splay, 7- abandoned channel, 8- fluvial terrace, 9- erosive areas, 10- stream, 11- abandoned channel, 12- maximum lake level, 13- alluvial fan, 14- fault, 15- delta distributary channels, 16- escarpment/ cliff, 17- contour line (redrawn from Emre et al., 1997).

Assos, Antandros, Bergama/Pergamon, Sardis, İznik/ Nikaia, Aydıncık/Kyzikos, İzmit/Nicomedia, and Bursa/ Prusias) developed throughout the Late Holocene in this region (Figure 1). On the other hand, the SDB, a very large area in the southern Marmara region, has remained nearly completely uninhabited for a long time. Between the end of the Late Bronze Age and the early Roman periods, from 1500 BC to 200 AD, the number of prehistoric and historic settlements seems to be low, even rare, when compared to other parts of Anatolia. Indeed, although corresponding to three-fourths of the whole surface of the southern Marmara region, the SDB today possesses only a few important ancient settlements, of which the best known are Prusias (old Bursa), Apollonia, and Daskyleion (Figure 1). This low population density in such a large area may find an explanation in causes related to lithology, watercourses, and landscape evolution. This low population density of a large area in the southern Marmara region in ancient times deserves an explanation, which could be achieved by a detailed study of the landscape evolution especially in and around Daskyleion as the key archaeological site in the center of the SDB, which could provide a correlation between landforms and land use in the region.

2. Geological and geographical settings

The southern Marmara region is a transition zone between active transform and extensional tectonic regimes controlled by the North Anatolian Fault (NAF) in the north and the Aegean grabens in the south (Figures 1 and 2) (Barka, 1997; Gürer et al., 2006, 2016; Emre et al., 2013). Many seismically active faults have caused devastating earthquakes (Şaroğlu et al., 1987; Kürçer et al., 2017). Moreover, Lakes Manyas and Ulubat are in a tectonic depression (Barka, 1997; Kazancı and Görür, 1997; Emre et al., 1998; Gürer et al., 2006) (Figures 2 and 3). Outcropping units from the Paleozoic and Mesozoic form the basement rocks of the metamorphic Uludağ Massif and Menderes Massif (Akyüz and Okay, 1998). The mountainous part of the SDB consists mainly of these older rocks (Figures 1 and 2). In contrast, Neogene units are composed of marl, claystone, and clayey limestones intercalated with evaporitic sediments and volcaniclastics that form a low relief (Emre et al., 1998; Helvacı and Orti, 1998). In addition, Quaternary deposits of the Marmara region consist of marine coastal, continental, and recent alluvium. These occur in patch-like exposures distributed in space according to their origins (Figure 2). Fossiliferous

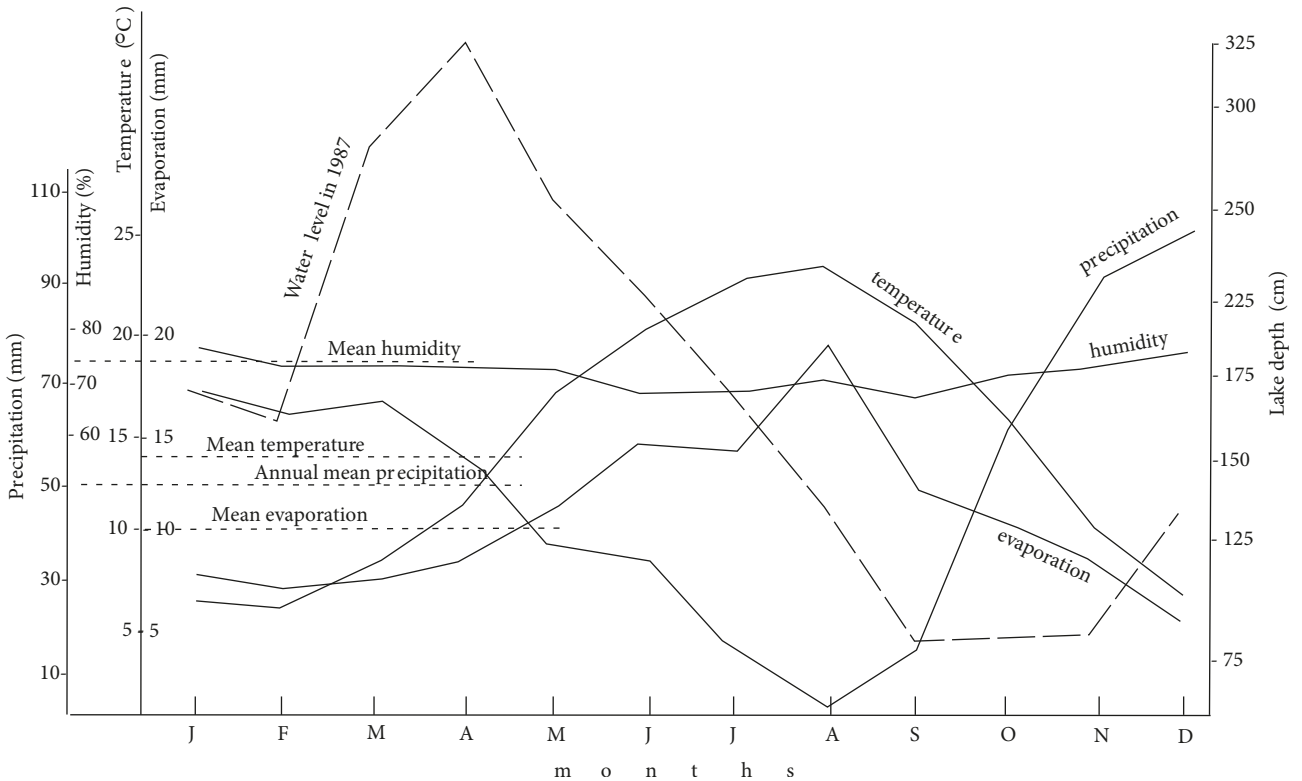

Figure 4. Long-time average of climatic values in the SDB compared to relative Lake Manyas level changes. Lake level is shown 5 years before regulation. Note that a one-month shift occurs between maximum and minimum lake levels with regard to the highest precipitation.

coastal facies, which are the key sites for the reconstruction of the opening and paleogeography of the Sea of Marmara, are beach-rock type marine deposits exposed on modern shorelines (Erinç, 1956; Erol, 1968; Sakınç and Yaltırak, 1997; Sakınç and Bargu, 1989; Görür et al., 1997). They rest unconformably on the Neogene units. Relatively younger clastic marine deposits form the deltas of the Gönen and Kocasu rivers (Kazancı et al., 1999). In particular, the Kocasu delta is unique as it is at the end of the Karacabey gorge where the Kocasu River reaches the sea (Erinç, 1957) (Figures 1–3). Significant continental Quaternary deposits are found in the Ulubat-Manyas depression. They have mostly a fluvial origin and they cover older units, mainly aged Middle and Late Neogene (DSİ, 1980) (Figures 3 and 5). All rock units in the area have been uplifted by tectonics and, as a result, are deeply incised by rivers. According to Kazancı et al. (2006, 2014), the erosion rate of boron beds in the Neogene deposits and the general morphostratigraphy of the region indicate that the morphology of the SDB formed during the last 300 ka.

2.1. Susurluk Drainage Basin

The SDB is drained by two streams, the Susurluk River and the Mustafakemalpaşa (MKP) River, and their distributaries (Figures 1 and 3). The basin, ca. 30,000 km^2, has a sharp and young topography declining from south to north. Altitudes, from the south in the highlands where they reach ca. 1300–1700 m a.s.l., with some peaks reaching >2000 m a.s.l. (upper SDB), change rapidly while descending to the lowlands (lower SDB) where they vary between 250 and 0 m (Figure 1). Consequently, the longitudinal profiles of streams are relatively steep, with turbulent waters carrying a significant amount of sediment load (Kazancı et al., 2004; see also a detailed topographic analysis in Kazancı et al., 2014). Highlands, which receive more precipitation than the annual country average, are densely covered by forests. However, the climate in the region is Mediterranean type (Figure 4). The number of villages is low in the highland, while the lowlands are densely occupied by farmlands and settlements of various sizes. Lakes Manyas and Ulubat and also the site of Daskyleion are in the lowlands of the SDB (Figures 1 and 3).

2.2. Lake Manyas

Lake Manyas, the first and most prominent Ramsar site in Turkey (wetland of international standard, recognized for its conservation importance), is a relatively shallow (maximum 10 m deep), freshwater reservoir of ca. 152 km^2 surface (Figure 3). Also known as a bird paradise, its formal name is Kuş Gölü ("Bird Lake"). Lake Manyas is

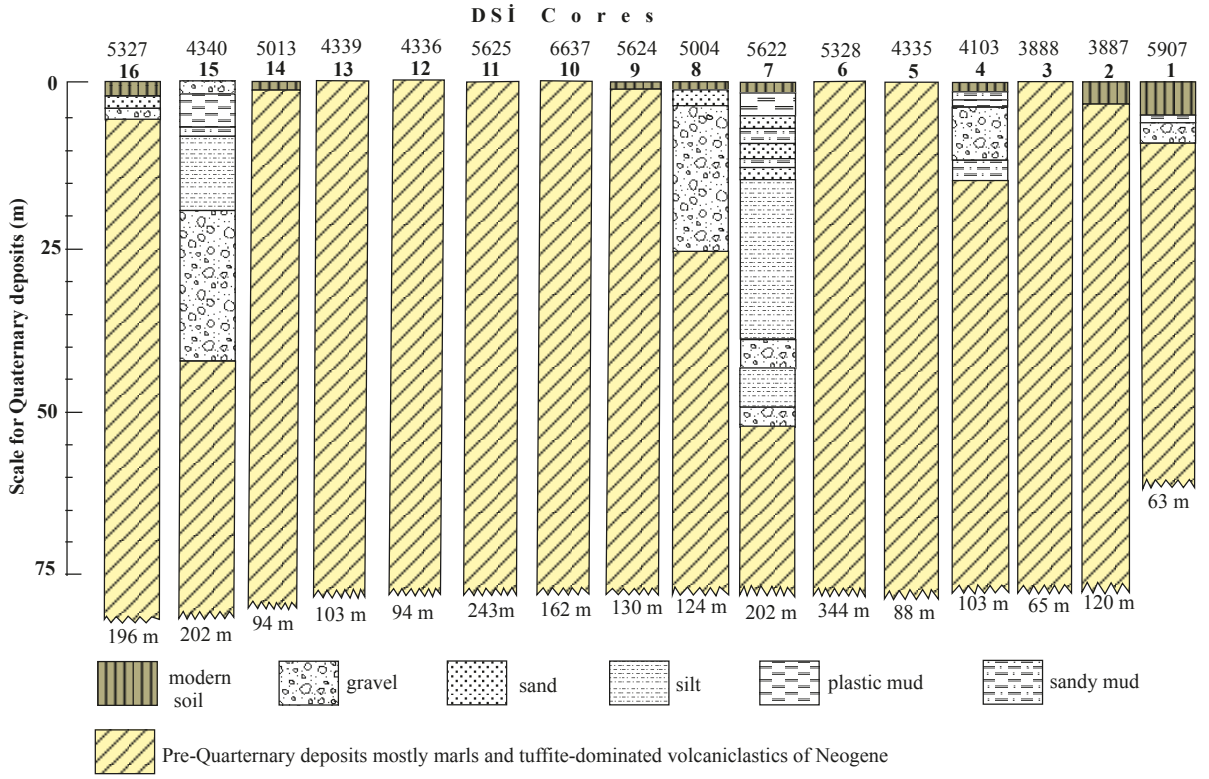

Figure 5. Logs of DSİ (State Hydraulic Works) cores. See Figure 3 for locations and Appendix for original codes in DSİ-1980. Note that Quaternary units are very thin. Only core 15 contains 42 m of Quaternary sediments.

highly sensitive to seasonal changes, typified by hot and dry summers and cold and rainy winters (Figure 4). At present the lake water is intensively used for irrigation. Its water level has been regulated since 1992 for this purpose and the outlet of the lake initiates the Karadere Stream, which flows just near the hill of Hisartepe (Figures 3, 6, and 7). The antique name of Lake Manyas was 'Daskylitis Lake' (Strabon, Book 12, Ch. 1.22; 8.10-11), after the name of King Daskylos, father of the Lydian King Gyges. Already then, it was described as a paradise due to its natural beauty (Herodotus, Book 3, Ch. 120, 126, B.6.33; Thucydides, B 1.129.1; Xenophon, Hellenica Book 4.1.15). At present, the water of the lake is of poor quality due to abundant fertilizer and insecticide use in the region (Erkmen et al., 2013). Moreover, its bottom sediment is resuspended on windy days, particularly in winter and spring when it is shallow. In relation to this resuspension, the modern sediment layer in the lake is a silt-dominated mud (Kazancı et al., 1997, 2004). Below the surface mud, an infill >10 m thick records an initial swamp phase during the late Holocene, later transformed into an open lake (Leroy et al., 2002).

2.3. Lake Ulubat

The general lacustrine characteristics of this lake are similar to those of Lake Manyas, except for surface morphology and partly its bedrock (Figure 2). It is a freshwater lake 120 km^2 wide, with a maximum depth of 7 m. It was also regulated in 1990. The main water source is the MKP River, which carries a significant amount of heavy metals and boron, as mines used to be active in the catchment (Kazancı et al., 1998, 2006). However, the heavy metal and boron content of the lake sediments (measured in the cored 7.8-m-long sequence) is low compared to its concentration in the water, most probably because of the wind effects accompanied by resuspension (Kazancı et al., 2010). Apollonia is the only ancient city close to the lake. It is built on Mesozoic limestones, which presented secure foundations for its earliest settlers (Figure 2). Lake Ulubat is also registered as a Ramsar site and is under official conservation.

2.4. Daskyleion

Daskyleion (also spelled Dascyleum and Dascyleion in some sources) is an ancient settlement built over the Hisartepe hill near Lake Manyas (Figures 1 and 3). It was the capital of the Persian satrapy that controlled Hellespontine Phrygia (modern southern Marmara region), and probably also Bithynia, Paphlagonia, Phrygia, and Cappadocia, in ancient Anatolia (Bakır, 2004, 2011). Its importance is also due to the succession of multiple cultures recorded in its ruins (e.g., Phrygian, Lydian,

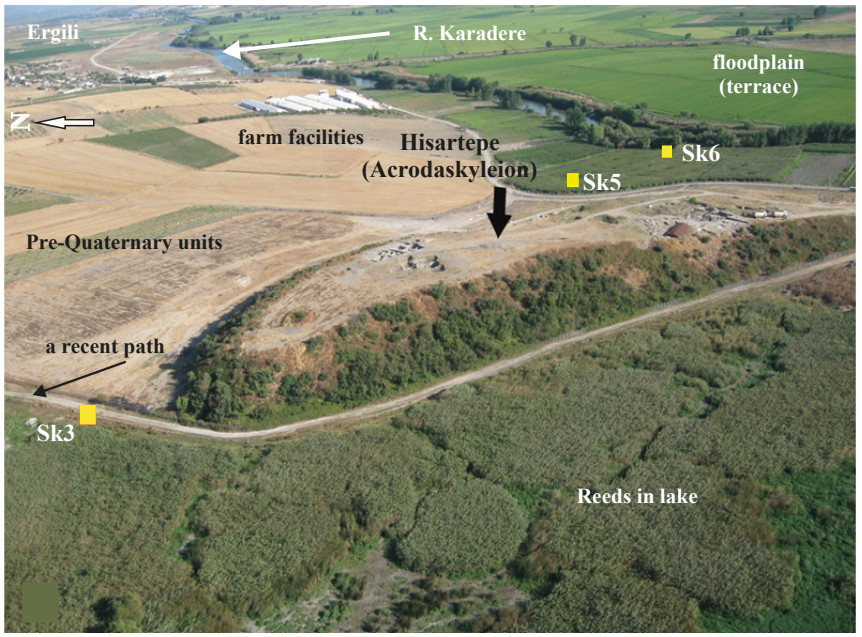

Figure 6. Hisartepe (Acrodaskyleion) and coring sites (SK3, SK5, SK6). Reeds in Lake Manyas are so dense that lake water is not visible. The recent path represents maximum water level just before regulation in 1991 (photo from Daskyleion Laboratory Archive).

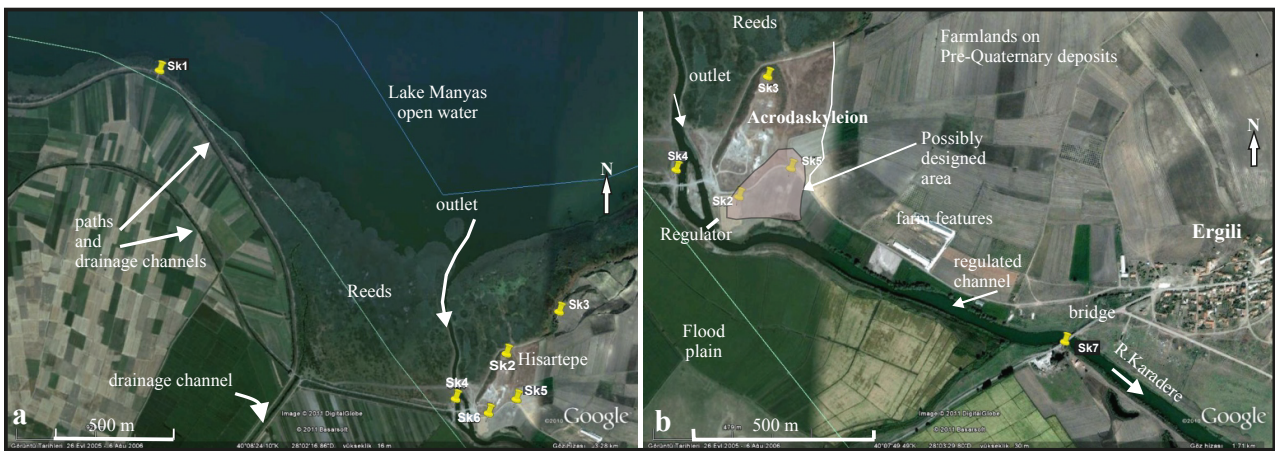

Figure 7. Close-up of the lake outlet, Hisartepe, and coring sites. a) Reeds concentrate at outlet where they are impacted by water fluctuation. Paths on the delta plain (left side of the photo) correspond to the borders of drainage channels. b) Outflow channel of Karadere River from Lake Manyas. Channel of this stream is still deepened from time to time due to siltation. Source: Google Earth, accessed in 2016.

and Persian) (İren, 2013). With the arrival of Alexander the Great in Anatolia in 334 BC, Daskyleion lost its fame and richness. After the second century BC, the settlement seems to have been deserted (Dereboylu, 2003). Further archaeological information about the city and excavation results can be found in the works of Bakır (2013), İren (2012), İren and Yıldızhan (2017), and references therein.

Hisartepe, the hill on top of which the Acropolis is positioned, is a 38-m-high hill close to the modern village of Ergili, on the southeastern coast of Lake Manyas (Figures 3, 6, and 7). The site was bounded by the lake and Karadere Stream (i.e. the lake outlet) (Figures 1 and 3). Such a confined location of a satrapy of the great Persian Empire in such a small area is explained by both security reasons—considering that about 1000 years later, the Byzantine army, searching for the best place for their military station, also choose the same hill (and the tell) to build a castle—and the presence of a beautiful

landscape with a fertile environment, commonly known as a paradise (Bakır, 2017, p. 3; Bulut, 2017, pp. 176-177; İren and Yıldızhan, 2017, p. 334).

3. Data acquisition

The main data sources for the present study are detailed geological and geomorphological maps of the lower SDB and 23 drill cores (Figures 3 and 5–8; Table 1). Original geological maps of the area were prepared by Emre et al. (1997). They are revised and reinterpreted here in light of lithofacies described based on core data. Core data can be separated into two sets. The first group, provided by the present study, is composed of seven cores (SK1–SK7) drilled around Hisartepe and near the artificial outlet of Lake Manyas (Figures 6 and 7). The second group consists of 16 core logs provided by the General Directorate of State Hydraulic Works (DSİ) (Figures 3 and 5). The cores around Hisartepe were obtained by engine-powered equipment with a core diameter of 72 mm. One of these cores (SK6) is 65 m long, while the other six are 20 m long (Figures 8a and 8b). They were retrieved during the summer of 2011 in order to detect the thickness of Quaternary lacustrine and fluvial deposits, the position and nature of the boundaries between Quaternary and Neogene units, and the paleotopography of the bedrock.

Locations, equipment, and recovery of the drillings were described in detail by İren et al. (2012) and Ergun (2013) (Table 1). Loose sandy layers, especially in core SK1, could not be fully recovered. For this reason, in this core, analyses of loss on ignition and measurements of magnetic susceptibility could not be performed (Figure 9). Sediments of all other cores were analyzed for mineralogy, geochemistry (organic matter, carbonate content, major and minor elements), and particle size by XRD, XRF, ICP-MS, sieving, and loss on ignition by routine techniques explained by Kazancı et al. (2010) in laboratories of Gebze Technical University, Acme Labs in Canada, Ankara University, and the General Directorate of Mineral Research and Exploration (MTA) (Appendices 1 and 2; Supplements 1 and 2; Figures 9 and 10). Because the sediments of the whole core of SK3 were analyzed at intervals of 10–20 cm, the results of only the upper 10 m are listed in Appendices 1 and 2. Bulk sediments of critical layers representing facies and/or environment changes have been dated by the ^{14}C technique using accelerated mass spectroscopy in the labs of Beta Analytic and calibrated according to Stuiver et al. (2017) with CALIB 7.1 (http://calib.org, accessed 2017-10-24) (Table 2). There are no palynological results for this study as no pollen or spores could be detected in most of the samples, probably because of oxidation. However, sediments of both Lake Manyas and Lake Ulubat are rich in palynomorphs (Kazancı et al., 1997, 1998, 2004, 2010; Leroy et al., 2002). Relevant results are used here for interpretations. Examination of the pollen content of the coal layer in core SK6 at depths of 45–48 m led to its likely attribution to a formation during the Pliocene (Figure 8b). These palynological results are not listed here as the age of the coal is outside of the scope of this study. Data from DSİ core logs correspond to 16 cores, which retrieved sequences between 63 and 344 m in length (Figures 3 and 5). Obtained during a regional survey performed for hydrogeological purposes (DSİ, 1980), they include informative data both for local stratigraphy and interpretation of Quaternary deposits (Figure 5).

4. Results

4.1. Characteristics and distribution of Quaternary deposits

Using our field observations, combined with the core logs drilled by both the DSİ and in this study, a geological and geomorphological map of the region was prepared (Figure 3). According to ^{14}C dates, most of the Quaternary deposits in the region belong to the Holocene (Figures 8a and 8b) (Table 2). Moreover, they form a "skin" of 5 m to 40 m on the peneplained late Miocene-Pliocene sequences and to a lesser extent on early Miocene and older bedrock (Figures 2, 3, and 5). In some localities around Lake Manyas, the lowermost layers of the Quaternary sediments are younger than mid-Holocene (Figures 8a and 8b). This observation suggests that the current morphology of the region reflects the early Holocene landscapes, together with lakes and river channels (Emre et al., 1997, 1998). In depressions and paleovalleys, the Holocene sediments are relatively thick (>20 m), but they are limited on the surface (Figure 5). Core SK1 (on the lake shore) is a typical example of such a >20-m-long core (Figure 8a). The Quaternary and/or Holocene sediments of it are composed of fine clastics, mostly silt and clay. The coarse-grained deposits are relatively scarce, but they are good indicators of channel migrations in the region. The oldest gravelly deposits of the Quaternary (dated as Middle Pleistocene by relative stratigraphy and/or superposition of Quaternary deposits), on which the town of Karacabey is settled, are relicts from a channel-fill (Figure 3). It was likely formed when the Manyas-Ulubat depression was a closed basin (Emre et al., 1997, 1998). Here, Quaternary deposits are loose and relatively dark in color because of its content in organic matter, in contrast with Neogene deposits, which are carbonate-rich marl intercalated with some limestone and gypsum layers formed in a lacustrine environment. Therefore, Quaternary and Neogene deposits can be easily differentiated by their color, both in surface exposures and in cores (Figures 2, 5, and 8). The internal organization of the Quaternary sediments is an alternation of cross-laminated sands and parallel laminated silt and clay beds, indicating that they were deposited in fluvial systems

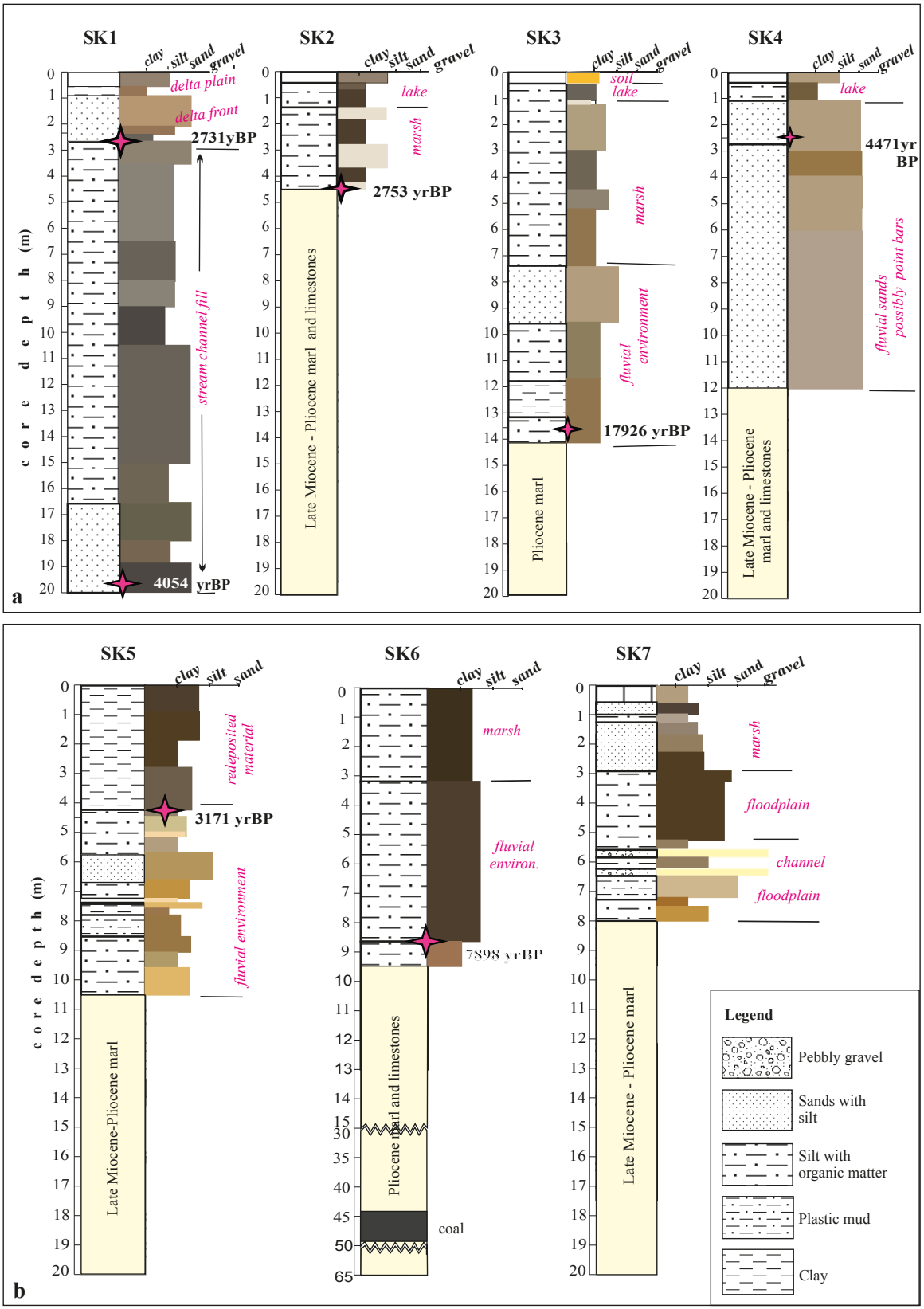

Figure 8. a, b) Logs and stratigraphy of cores SK1-SK7. The ages on columns are calibrated years BP, with reference to 1950. See Table 5 for detail of the dates.

Table 1. Coordinates of cores SK1-SK7.

	SK1	SK2	SK3	SK4	SK5	SK6	SK7
Latitude Longitude Elevation (m a.s.l.)	40°14′73.57″ 28°02′59.57″ 17.15	40°13′40.89″ 28°05′11.13″ 24.20	40°13′62.70″ 28°05′45.24″ 19.00	40°13′13.27″ 28°04′79.25″ 16.30	40°13′11.57″ 28°05′24.03″ 19.10	40°13′05.74″ 28°05′03.30″ 17.25	40°12′74.36″ 28°06′23.79″ 18.25

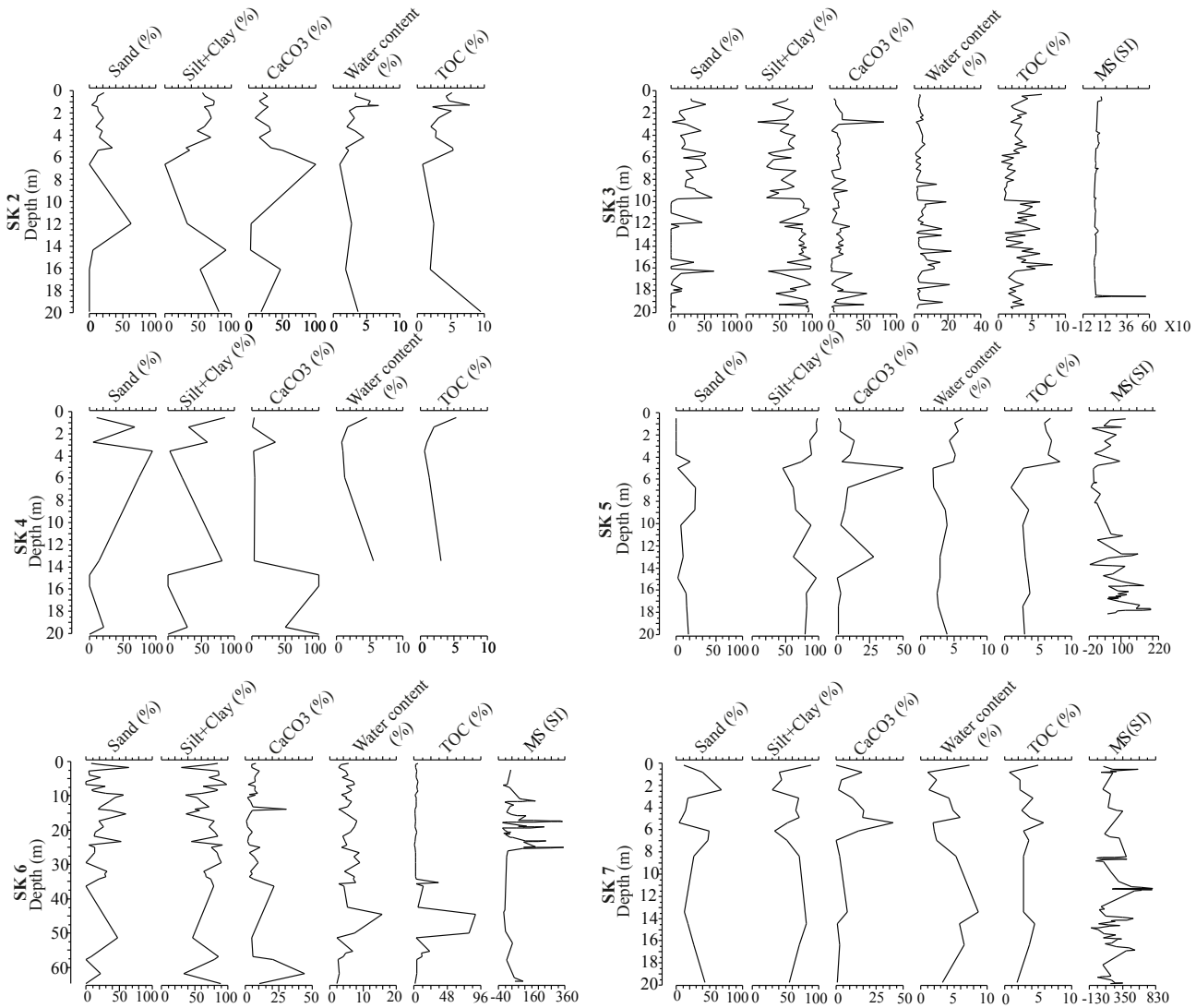

Figure 9. Grain-size characteristics, carbonate and organic matter content, and magnetic susceptibility curve of cores SK2 to SK7. Compare with Figures 8 and 12. See Table 1 for the metric levels of core sediments analyzed. Note that samples intervals are not the same for all cores due to technical difficulties.

(i.e. in channels, floodplains, and also in delta plains; Reineck and Singh, 1980; Allen, 1984). At present only stream channels are active in the modern depositional environments, because they concentrate impacts of intensive anthropogenic activities. In particular, artificial drainage channels have deeply modified the area (Figures 3, 6, and 7).

4.2. Stratigraphy of Quaternary deposits

The general stratigraphy of the Quaternary sediments in the SDB is simple to describe, as the thickness is limited,

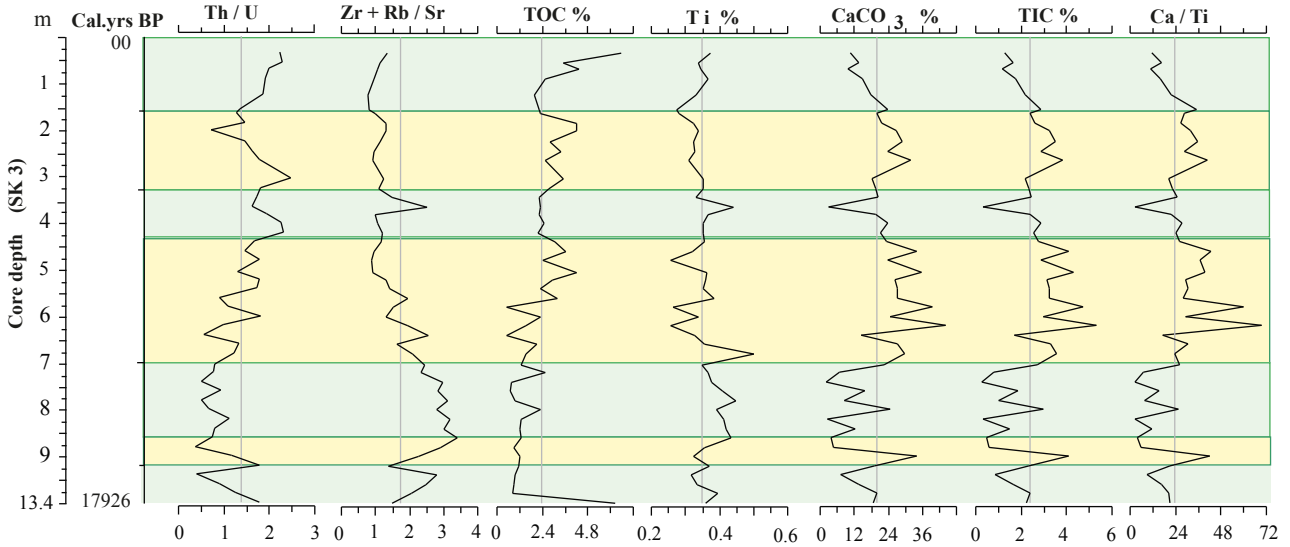

Figure 10. Environmental parameters of the SDB from core SK3. See Tables 3 and 4 for the analytical results. Note that values here belong only to the Holocene part of the succession. Gray and yellow intervals represent wet and dry climatic periods. See Figure 8 for core log and lithostratigraphy.

Table 2. Radiometric dates from cores retrieved around Lake Manyas (calibration: Stuiver et al. 2017; CALIB 7.1 at http://calib.org, accessed 2017-10-24).

Core site	Laboratory number	Sample name	Comp. depth in cm	Material dated	Age	Cal. AD age ranges	Median probability AD/BC	Cal. age, year BP
Ulubat	Poz-3638	AK11/770-80	619	Seeds	1612	Cal. AD 391- 537	459	1491
Ulubat	Poz-3636	AK11/820-30	677	Twig	1708	Cal. AD 314–396	341	1609
Manyas	Poz-3646	ML1/444-47	319	Seeds	1545	Cal. AD 426–572	487	1463
Manyas	Poz-3647	ML1/441-44	322	Seeds	1556	Cal. AD 422–567	485	1465
Manyas	Beta-146142	ML11/590-100	409	Seeds	1710	Cal. AD 242–409	332	1628
Manyas	Beta-312029	SK1-24	240	Organic sediment	2570	Cal. BC 808–749	–781	2731
Manyas	Beta-312031	SK2-42	420	Organic sediment	2620	Cal. BC 829–776	–803	2753
Manyas	Beta-312034	SK5-45	450	Organic sediment	2990	Cal. BC 1299–1119	–1221	3171
Manyas	Beta-312030	SK1-199	1990	Plant	3720	Cal. BC 2201–2032	–2107	4054
Manyas	Beta-160591	ML11/110-10	1080	Twig	3750	Cal. BC 2235–2035	–2162	4112
Manyas	Beta-312033	SK4-26	260	Organic sediment	3980	Cal. BC 2577–2457	–2521	4471
Manyas	Beta-312035	SK6-82	820	Organic sediment	7070	Cal. BC 6022–5877	–5948	7898
Manyas	Beta-312032	SK3-135	1350	Organic sediment	14730	Cal. BC 16176–15752	–15976	17926

generally less than 40 m (Figures 5 and 11). However, determining the age of this sediment is important, not only for paleogeography but also for determining the evolution of the two lakes. Sediments from cores SK1 to SK7, being well preserved and providing detailed stratigraphy, have been ^{14}C dated (Table 2; Figures 8a and 8b). The longest core, SK6, reached a Neogene coal layer (low calorific lignite) at a depth of 44–51 m (Figure 8b). According to the pollen content of this coal layer, this part of the sequence dates back to the Pliocene.

Dates from the core sediments around Lake Manyas show that Quaternary sediments are about 5–20 m thick and only a few can reach the late Pleistocene (Table 2). Their age is generally middle to late Holocene, with only one core (SK3, at the northern foot of Hisartepe) covering the whole Holocene time span (Figures 8a and 8b). However, there are other Quaternary sediments in the SDB, whose ages are out of reach of the ^{14}C dating method, such as some gravelly layers around Lake Ulubat and the town of Karacabey, which have been suggested to be aged middle Pleistocene (Emre et al., 1997, 1998) (Figures 3 and 5). In addition, the lacustrine muds from Lake Manyas and Lake Ulubat point to a parallel chronology of both core sequences at two depths: sediments of ca. 10.8 m in depth are 4.2 ka cal. BP old, while at 6.77 m they are 1.7 ka cal. BP old (Leroy et al., 2002; Kazancı et al., 2010) (Table 2).

Radiometric ages of some layers allow the calculation of deposition rates for the relevant intervals in the sediment succession. The calculated average sedimentation rates are 1.32 and 0.08 cm/year for fluvial and lacustrine deposition in core SK1 (Lake Manyas) (Figure 11). The 0.15 cm/year sedimentation rate evidenced in the lacustrine interval in SK2 corresponds to nearly double the value of that obtained in SK1 (0.08 cm/year) (Figures 8 and 11). These results were not used for interpretations because sediment transportation is more rapid and irregular in channels or meandering streams than sediment deposition occurring in open lakes. On the other hand, geochemical results show clearly alternations of dry and wet climatic periods during the deposition; however, these periods were not dated in this study (Figures 10 and 11).

4.3. Mineralogy and geochemistry

Grain size, mineral composition, calcium carbonate, total organic carbon, and magnetic susceptibility (MS) of the whole core sediments are presented, together with details of the major and mineral element constituents of the 10-m-long core SK1, in Figure 9 and Supplements 1 and 2 (see also Appendices 1 and 2). The lithology around Hisartepe, including that of Pliocene age, is relatively fine-grained. However, the older deposits include limestone layers, characterized by high values of calcium carbonate (Figure 9). Fine pebbles and sand layers occurring in the youngest deposits of the late Quaternary are interpreted as channel fills. Common particle sizes are silt and clay, as expected from flood plains and marsh sedimentation environments (Figures 8 and 9). A significant difference between sediments of Pliocene and Quaternary ages seems to be the high MS of older ones. The mineral assemblage of the Quaternary deposits is mainly composed of illite, quartz, plagioclase, and calcite (Supplement 1). Quartz and feldspars are abundant in the sandy layers. Illite and calcite occur in the muddy layers and are interpreted as flood-plain, marsh, and lacustrine sediments (Figures 8a and 8b; Supplement 1). This confirms that sediments derive from the same parent rock in the upper SDB. Total organic carbon increases in some layers, particularly in the upper levels of cores SK2, SK3, SK4, and SK5, where the increase occurs more or less in parallel with increase in water content, due to probably organic matter affecting the porosity (Figure 9). The elementary composition hardly changes between levels, as it is dependent on the mineral composition of the sediment. However, ratios of Th/U, Zr+Rb/Sr, and Ca/T provide evidence of variability between levels (Figure 10; Supplement 2).

5. Discussion

The Quaternary landscape evolution in the SDB can stand as a reference for the whole northwestern Anatolia as geology (as well as the particularly tectonic regime) is more or less the same in the region. Stratigraphy and chronology results show that the study area was exposed to intensive erosion during the Pleistocene until the end of the LGM, with only the Holocene deposition preserved in the Manyas-Ulubat depression and at the base of some deeply incised river valleys. It should be reemphasized that one of the controlling factors on this development was base-level changes and/or water level fluctuations of the Sea of Marmara (Çağatay et al., 2003, 2006, 2009; Eriş et al., 2007, 2010).

Three types of erodible lithology are found in the region. These are soft sediments of the Quaternary fluvial dynamics, clay-dominated Neogene rocks, and hard but altered rocks of Mesozoic and Paleozoic ages. The Quaternary deposits generally occur on the plain surfaces at elevations of 0–250 m a.s.l. (Figure 3). The Neogene units, mostly consisting of marl and to a lesser extent gypsum, limestone, and fine-grained volcaniclastic rocks, form the main lithologies in the lowlands. The highlands, above ca. 1250 m altitude, are formed of sedimentary, magmatic, and metamorphic hard rocks, which are all highly weathered (Helvacı and Orti, 1998; MTA, 2002) (Figure 2). Neogene units and older altered rocks in the highlands are highly disintegrated and less resistant to erosion, such that large valleys could develop in the basin (Helvacı, 1984; Kazancı et al., 2014). Moreover, the erodible lithology provides a large amount of sediment

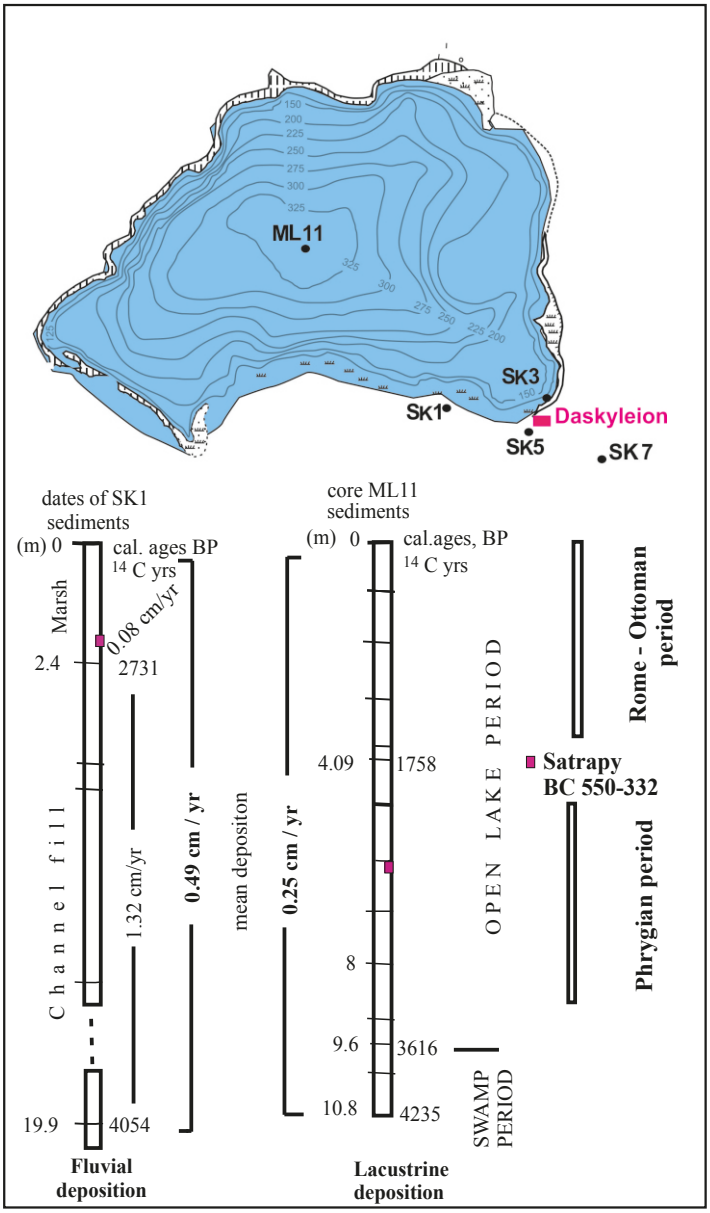

Figure 11. Correlation of deposition in lakes and flood plains together with history of Lake Manyas evolution, according to pollen content studied by Leroy et al. (2002).

load to the streams, causing downstream the formation of deltas in the lakes and the Sea of Marmara (Kazancı et al., 1999, 2004). The erodible nature of the Neogene rocks also generated a smooth morphology in the region, characterized by low relief and low-angled slopes (Kazancı et al., 2014). The result of a high rate of erosion is a high rate of sedimentation in reservoirs, i.e. in either natural or artificial lakes by damming of fluvial channels. Thus, in the SDB, the overall rate of fluvial sedimentation during the Holocene in valleys is lower, according to core dating, than the rate recorded in lacustrine sedimentation in and around the Manyas and Ulubat lakes (Figure 11).

5.1. Development of Lakes Manyas and Ulubat

Geomorphological analyses (Emre et al., 1997, 1998) suggest that Lake Ulubat and Lake Manyas formed in response to a combination of tectonic and fluvial processes in a seismically active depression between Gönen and Karacabey (Figure 2). The results above also show that both lakes appeared in the late Holocene (Figures 8 and 12), which is the last stage of landscape evolution in the region.

Together with a smooth morphology, the land surface was lower than the present one by the end of the Neogene, permitting the formation of lacustrine and pyroclastic

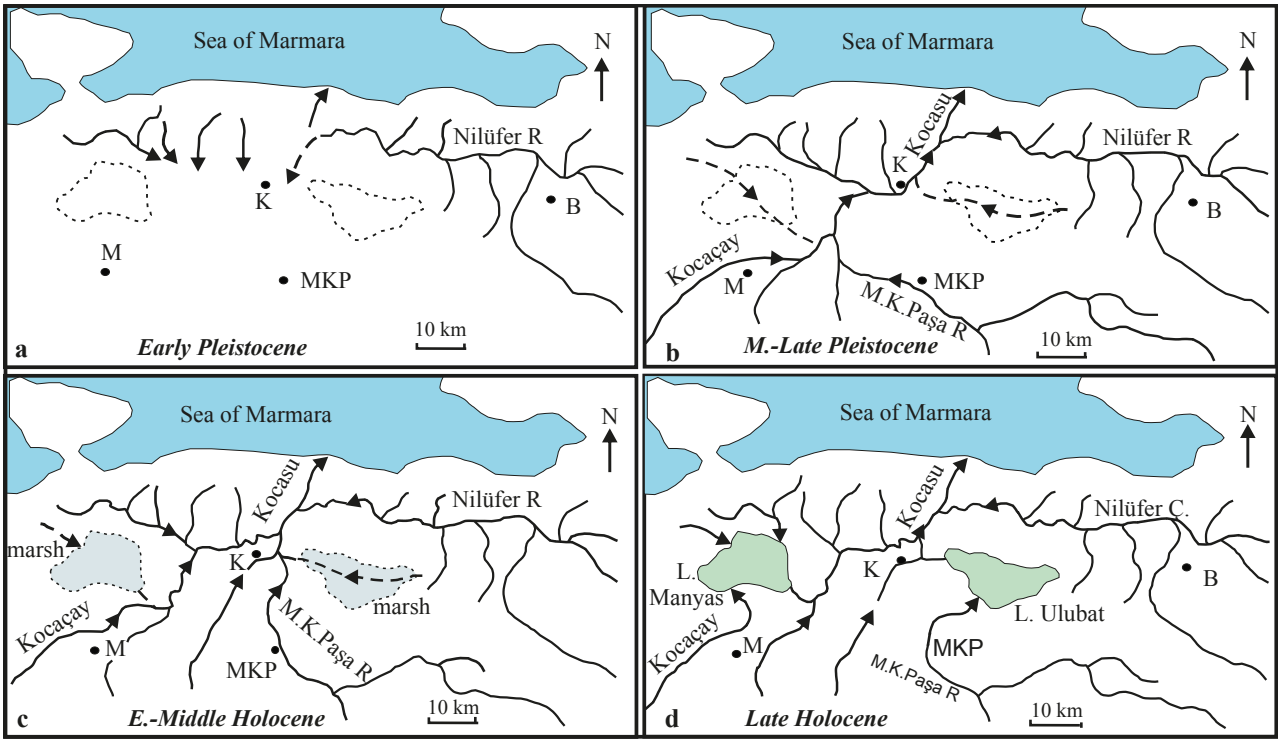

Figure 12. Stages of formation of Lakes Manyas and Ulubat (from Emre et al., 1997). Names of settlements are abbreviated by capital letters. Arrows show flow direction of streams. a) Early Pleistocene; only R. Nilüfer can be identified, and the SDB is a closed basin. b) Middle to Late Pleistocene; the SDB becomes open to the sea. c) Early-Middle Holocene; the sea level rises, forcing the meandering of channels in river flood plains; Lakes Manyas and Ulubat form behind large point bars built and abandoned by the moving meanders. d) Late Holocene; marshes change to fresh water lakes. B = Bursa, K = Karacabey, M = Manyas, MKP = Mustafakemalpaşa.

units of Late Miocene-Pliocene age (Figure 13). Tectonics then became active, creating high relief contrast with hills and depressions. At the end of the Middle Pleistocene, the Manyas-Ulubat depression was still a closed basin with, possibly, an antecedent stream flowing in from the southern part of the Karacabey gorge (Emre et al., 1998). Some relicts of compacted gravels exposed near the town of Karacabey and south of the town of Manyas prove that the Manyas-Ulubat depression became an external drainage basin in the Late Pleistocene (Figures 3, 12, and 13). During that time, strong erosion removed nearly all Pleistocene deposits from the highlands and lowlands, preserving only a few exposures of compacted coarse-grained gravel (Figures 3 and 13). Together with the DSİ's cores, the seven SK cores, six of which reached Neogene units in and around Lake Manyas, provide a reliable landscape scenario for the Quaternary (Figures 3, 5, 7, and 8). Published core analyses for Lakes Manyas and Ulubat (Leroy et al., 2002; Kazancı et al., 2004) were used to check and compare the results. Finally, we suggested that Lake Manyas was originally a swamp (Figures 11 and 12), located most probably beside a meandering channel, possibly as a shallow ox-bow lake created by an abandoned channel as suggested by Emre et al. (1997). Meanwhile, incised fluvial channels near the swamp/lake areas were filled, as detected in core SK 1 (Figure 8a). Similar incisions and infill records are also recorded in DSİ cores (Figure 6). Incisions are interpreted as a fluvial response to the water base-level falling, during the LGM, to 130 m below the present sea level in the Marmara Sea basin, which was then occupied by a large lake (Emre et al. 1997, 1998; Görür et al., 1997; Ryan et al., 1997; Çağatay et al., 2000, 2003, Eriş et al., 2010). However, these incisions are relatively small and young when compared to the deep, canyon-like valleys in the upstream parts of the river network. These were partly formed most probably during the Middle Pleistocene (Kazancı et al., 2014). Because of the rapidly rising sea level in the Early and Middle Holocene, fluvial sedimentation became dominant in the downstream parts of the river courses in the SDB where a multiple meandering channel system expanded (Figures 11 and 12). The Sığırcıdere was captured by a local stream and turned to the south (Figure 3). Near Hisartepe, a large-point bar developed in the meandering channel of the Kocaçay River (and Karadere), causing the formation of a swamp area transformed into Lake Manyas ca. 4000 years cal. BP (Figures 11 and 12). At first, the lake was about half its present size, before it enlarged over time toward the south

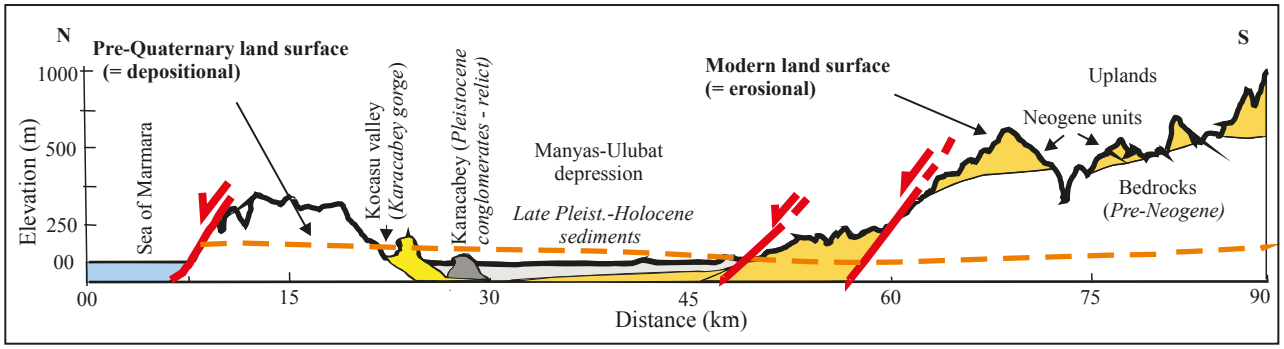

Figure 13. Geomorphological cross-section of the SDB in N-S direction. See Figure 2 for location. The land surface morphology at present has been formed by effects of a combination of tectonism and earth-surface processes. Yellow line indicates a surface transition between Pliocene and Pleistocene, which shows that the Sea of Marmara did not exist at the end of the Pliocene.

and the west, as shown by the northward progradation of the Kocaçay delta (Figures 1, 3, and 12). Hisartepe, which is an erosional remnant of Neogene units (Figure 6), seems to have been one of the factors controlling this fluvial development, with its N-S trending morphology and limestone-supported lithology. While bounding the lake on its western shore, it also provided an elevated land connection to the bedrock in the north. Similar lacustrine development occurred in Lake Ulubat where the MKP River also formed a delta in the southwestern part of the lake (Figures 3 and 12). Lakes Manyas and Ulubat, as well as their associated shallow wetlands, are thus young, dating as Late Holocene. Today, they are still a significant part of the local geography and landscapes (Figure 3). Reference timing and corresponding sediment thickness used for calculating the deposition rate were the year 1950 and ground surface below lake level, respectively. See Table 1 for the coordinates of cores SK1 to SK7. Results from SK1 indicate the irregularity of deposition in fluvial environments (Figure 11).

5.2. Fluvial control on the land

The second important geomorphic process in the SDB was the rapid change of river systems that controlled past and present land development. Parallel to the formation of the lakes, the main fluvial event was the lateral migration of channels and related floodplain formation in valleys in the Ulubat-Manyas depression. The imprint of abandoned channels is still visible in the landscapes (Figures 3, 6, and 7). A typical example is the Mürüvvetler River, whose course makes a bend to the northeast before reaching the Karadere (Figure 3). However, in the past it used to flow into Lake Manyas to the west of Esenköy, according to distribution of older channel deposits in the field (Figure 3). The Susurluk River also changed its course toward the north at Çeltikçi, when it was a tributary of the MKP River along the Çeltikçi-Güllüce valley. In fact, the Güllüce valley was a deep incision that was filled in the Holocene (Figures 3 and 5; core DSİ 15) (Emre et al., 1997). The other example of river network change is the capture of Sığırcıdere by Lake Manyas (Figure 3). This capture is recorded in old terraces and relict alluvium evidencing that the old Sığırcıdere was some time ago outflowing to the Sea of Marmara, where it used to meet the Karadere River's mouth near the village of Tophisar. The exact causes of these channel diversions are not obvious. They may have been caused either by tectonics or high sediment load, or, most probably, by the combined impacts of both event types (Figure 12). During the late Holocene, the lower SDB was flooded by a high volume of surface and ground water that created large marshy flood plains (Figures 3, 14, and 15).

Alternations of clayey and sandy layers in the sediments indicate flood occurrences, i.e. the construction of the flood plain in a river system. Because of the relationship between the drainage area and the flood plain downstream, these alternations may point to a climatic record of the basin during the time of the flood plain aggradation. However, the occurrences of rapid climate changes in the Holocene in the eastern Mediterranean region are documented (Roberts et al., 2001; Mayewski et al., 2004).

Changes of some elements and element ratios through sediment successions provide information about relative changes in a climate context (e.g., Dypvik and Harris, 2001; Haberzetti et al., 2007). In order to obtain evidence for possible changes, for core SK3, values of Th/U, Zr+Rb/Sr, TOC (total organic carbon), Ti, $CaCO_3$, and Ca/Ti ratio of the sediment were calculated and results were interpreted for the possible paleoclimate of the Holocene (Figures 9 and 10; Table 2; Supplement 2). Generally it is accepted that Th/U, Ti, Zr+Rb/Sr, and TOC increase during wet periods, while $CaCO_3$, TIC, and Ca/Ti decrease (Jones and Manning, 1994; Dean, 1999; Meyers and Lallier, 1999; Wojciciki and Marynowski, 2012). In addition, an increasing clay and/or silt+clay ratio is an indication of a wet climate. Their values in the studied sediments are more or less parallel with those of TOC and Th/U (Dypvik and Harris, 2001; Haberzetti et al., 2007; Ülgen et al.,

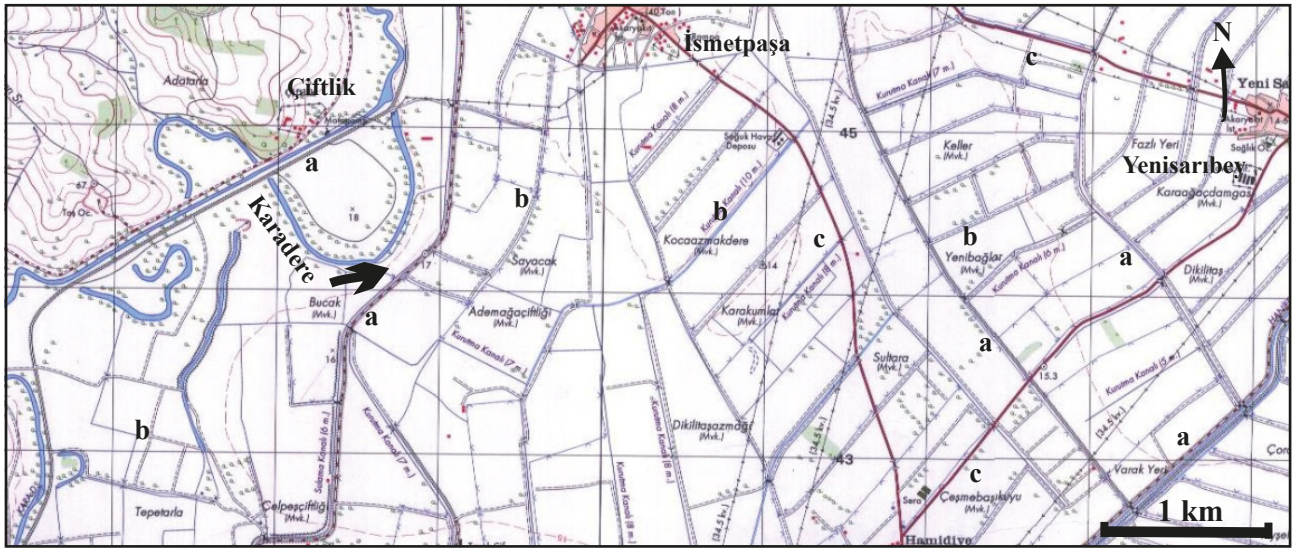

Figure 14. Anthropogenic influence on the land. People (mostly immigrants) constructed many drainage channels in order to gain fields for farming with the help of the state between 1950 and 2000. a) Irrigation channels, b) drainage channels, c) asphalt roads. There are earth roads along all channels. See Figure 3 for location of the area. Source: Topographic map at scale 1/25,000, prepared and printed in 2001 by General Directorate for Charts of the Turkish Army, Ankara.

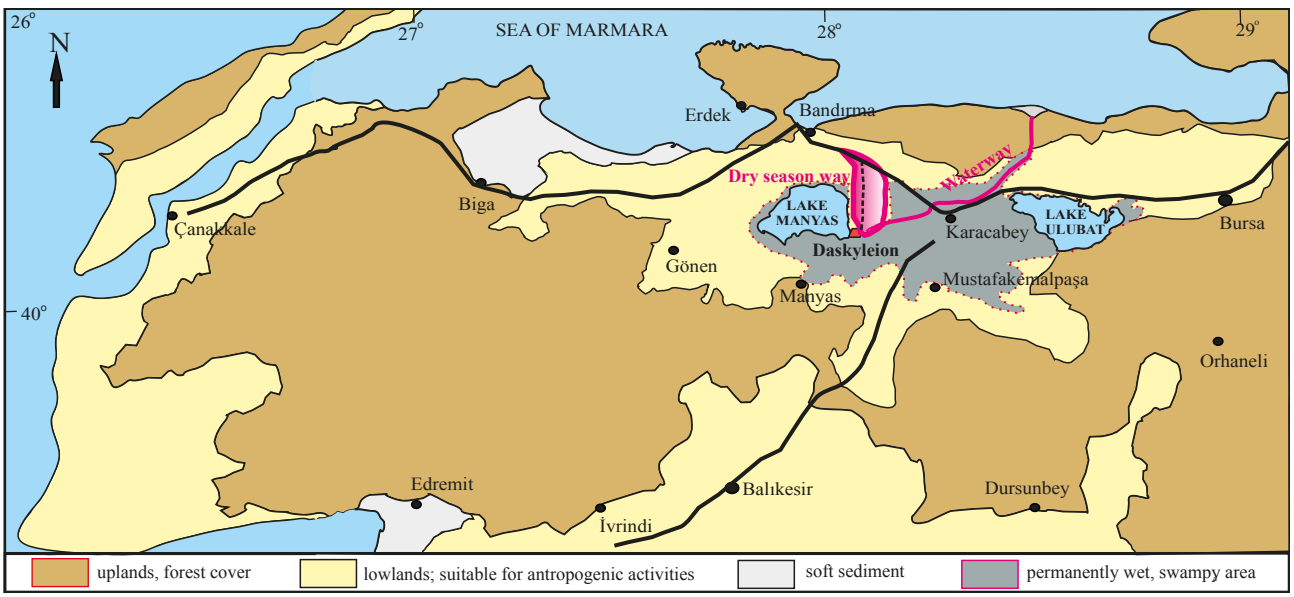

Figure 15. Suitable and unsuitable areas for settlements in the southern Marmara region based on lithologies and ground water level. Note that suitable areas frequently correspond to Neogene, mostly pyroclastic rocks. The Quaternary part of the lowlands of the SDB have remained permanently muddy (unsuitable) during the last three millennia according to our interpretation based on lithology and geomorphology. Other Quaternary areas (soft sediment in the legend) may have been muddy, but we have no data. Compare with Figure 3. During and since the Iron Age, Daskyleion could be reached both by land and by waterway (Karadere) from the main road (black line). According to antique (Roman) sources, this road was used since the Early Iron age (https://omnesviae.org). Pink area shows possible connections of Daskyleion with its surrounding land; however, very recent erosion and land transformation by man have erased all signs of it, if any.

2012) (Figures 9 and 10). Based on these references and analytical results, it possible to say that Holocene climatic fluctuations were recorded in the sequences studied here. However, reliable age data and more analyses are needed for further interpretations (Roeser et al., 2012; Miebach et al., 2016). Wet and dry intervals of Holocene climate

have been already presented for other parts of Anatolia by previous studies (i.e. Lemcke and Sturm, 1997; Eastwood et al., 1999; Kuzucuoğlu et al., 2011; Roberts et al., 2011).

5.3. Daskyleion and settlements in the southern Marmara region

The number of prehistoric and historic settlements in the southern Marmara region is unusually small compared to other regions in western Anatolia (Figures 1 and 3). However, the area is now highly populated (TÜİK, 2016) and even redeveloped (Figure 14). One of the reasons for the present situation is forced mass migrations from the Balkans in the 19th and 20th centuries and then during the Cold War (Halaçoğlu, 1995). The natural advantages of the region for settlement are 1) proximity to the seas, particularly to the straits of İstanbul and Çanakkale; 2) the abundance of lowlands for agriculture; and 3) the abundance of water sources. Such places are attractive for living, not only today but also in the past (i.e. Baltacıoğlu, 2005, p. 6; Öziş, 2015). It is supposed that the location of Daskyleion has more to do with the low settlement density in the region rather than local advantages. The natural beauty and profusion of wild animals were additional reasons (Bakır 2011, p. 58, p. 69; İren and Yıldızhan, 2017, p. 334). Lake Manyas must have provided a safe boundary for the satrapy (Figure 6). However, the site was confined by the lake and the Karadere Stream, both of which are a source of a plethora of mosquitoes, even today. According to genetic studies on the Mediterranean anemia transferred to man by mosquitos, anemia had been a serious health problem during the Neolithic and Chalcolithic in the Middle East (Le Mort et al., 2006) and also in Egypt (Hume et al., 2003; Smith, 2015). Thus, there must be another reason not to attract people to settle here. The results of this study suggest that the main reason for Daskyleion's first settlers to select Hisartepe was to avoid the fine-grained lithology of the surrounding land (Figures 10 and 14). According to sediment characteristics and radiometric dates, between 1500 BC and 500 AD, the lowlands of the SDB were covered by marshes and/or permanent swamps related to the flooding of many streams flowing into the depressions in the lowlands (Figures 3, 6, 10, 13, and 14). Areas with relatively high altitudes, such as Hisartepe and other hills in its eastern and northern surroundings, were safe from floods. Other areas such as some clayey Neogene outcrops were muddy in rainy seasons; however, they were dry for some part of the year, thus remaining relatively suitable places for daily life. In addition, the Daskyleion location permitted two safe connections with other cities, such as through the Karadere waterway to Kyzikos near Lake Ulubat, and harbor cities located along the Sea of Marmara through a north-trending strip of land connection (Figure 15). Other settlements in the SDB, such as Karacabey (Kremastis) and Gölyazı (Apollonia) village, were on relatively high and dry grounds (Figures 2 and 15). Similarly, all old cities in northwestern Anatolia, e.g., Bursa, Troy, Kyzikos, and Bergama, were built on solid rocks that were safe from flooding during wet seasons (Figures 1–3). This approach of selecting solid ground for housing lasted up to the middle of the 20th century in Anatolia, leaving lowlands for agriculture and animal husbandry when possible. However, recently wet plains and marshes have been drained by trenches in addition to the deepening of natural channels to prepare and expand lowlands for settlements for people who had to migrate from the Balkans (Halaçoğlu, 1995; Kaplanoğlu, 1999; Özcan, 2016) (Figure 14). Together with migration from outside, the southern Marmara region is now the most populated area of Turkey (TÜİK, 2016).

6. Conclusions

The results of core examinations combined with geological and geomorphological studies provide information about the Quaternary evolution of NW Turkey. The whole southern Marmara region slopes down northwards and is drained by the Biga, Gönen, and Kocasu rivers (Figure 1). The latter river and its tributaries (Kocaçay, Simav, Mustafakemalpaşa, and Orhaneli streams) collect water from the SDB, an area of ca. 30,000 km^2. This flow is directed to the Kocasu delta, which extends into the Sea of Marmara (Figures 1 and 3). Maps and cores on the lower SDB indicate that the Quaternary deposits are not distributed locally; most often, they occur as a cover ca. 10 to 40 m thick (Figures 2, 5, and 8). Neogene units, particularly sedimentary rocks of the Late Miocene-Pliocene and underlying fine-grained pyroclastics, have been largely exposed, forming a new land surface (Figures 2 and 13). It seems that intense erosion occurred in the Quaternary after the uplift of lacustrine units, which started at the turn of Neogene/Pleistocene. From the relicts of both Pleistocene conglomerates at Karacabey town and the capture of Sığırcıdere by Lake Manyas (Figures 3 and 13), we conclude that the intense erosion period was contemporaneous with increased tectonic activity during the Middle and Late Pleistocene. Such a combination of processes also controlled the formation of the Kocasu delta (Figure 3). Formation and development of Lakes Manyas and Ulubat was the last stage of the land evolution in the southern Marmara region. Both lakes formed because of the damming of the Kocaçay and Mustafakemalpaşa rivers, constrained by a fault line rupture combined with a barrier uplift in the seismically active depressions where the lakes are positioned today (Figure 13). Damming of rivers and consequent changes in fluvial processes was particularly efficient on water accumulation behind the uplifted ridge from the start of the Sea of Marmara level rise in the Late Glacial.

However, it should be reemphasized that tectonics have been primary and regional factors in the geomorphic development of the region since the Middle Pleistocene.

Based on a combination of geomorphological, sediment core, and archaeological studies, lithology contrasts and recent environmental changes seem to have primarily controlled the distribution of short- and long-lived settlements in the southern Marmara region of Turkey. Lowlands of the SDB are clearly not favorable for settlements since the middle or late Holocene, with a few exceptions such as the satrapy capital of Daskyleion, which, built on a rocky outcrop, was preserved from the high water table in the surrounding marshes recorded by rather thick muddy sediment units (Figures 14 and 15). The current dense population is a very recent feature of the region. From another perspective, the present changes of marshes to arable agriculture areas in the SDB reflect not only anthropogenic effects on the land but also the efforts of immigrants to make a new country to live in despite an initially harsh environment.

Acknowledgments

This study was a part of the geological survey of Project 109K363 supported by the Scientific and Technological Research Council of Turkey (TÜBİTAK), coordinated by Kaan İren. This project also provided the material of the MSc thesis of Zeynep Ergun. Cores SK1-SK7 were extracted graciously by the Balıkesir Branch of the DSİ in 2011 under the supervision of Dr Nazif Demir. For its generous logistic and financial support, Kaan İren also thanks the Muğla Sıtkı Koçman University Funds (BAP) and the Ministry of Culture and Tourism. Mehmet Tarık Özcan gave great support both in the field and laboratory. Dr Kıymet Deniz helped in performing geochemical analyses. Dr Esra Gürbüz made some topographical analyses and drafted Figure 2. Three additional dating results were obtained thanks to the financial contribution of the Ankara University Scientific Research Funds (Grant No: 12B4343002). Three anonymous reviewers of the journal improved the manuscript significantly. The authors are grateful for all the support and contributions.

References

Akyüz HS, Okay AI (1998). Manyas güneyinin (Balıkesir) jeolojisi ve mavişistlerin tektonik konumu. Maden Tetkik ve Arama Dergisi 120: 105-120 (in Turkish).

Allen JRL (1984). Sedimentary Structures; Their Character and Physical Basis I + II, 1st Edition, Development in Sedimentology 30. Amsterdam, the Netherlands: Elsevier.

Ardel A (1954). İznik depresyonu ve gölü. İstanbul Üniversitesi Coğrafya Enstitüsü Dergisi 5-6: 225-229 (in Turkish).

Ardel A (1960). Marmara bölgesinin yapı ve reliefi. Türk Coğrafya Dergisi 20: 1-22 (in Turkish).

Ardel A, İnandık H (1957). Marmara Denizi'nin teşekkülü ve tekamülü. Türk Coğrafya Dergisi 17: 1-19 (in Turkish).

Bakır T (2004). Daskyleion'da Phrygler. In: Korkut T (editor). Fahri Işık'a Armağan Kitabı. Antalya, Turkey: Ege Yayınları, pp. 55-67 (in Turkish).

Bakır T (2011). Daskyleion; Balıkesir'in Eski Çağlar'daki Valilik Merkezi. Balıkesir, Turkey: Balıkesir Valiliği İl Özel İdaresi Yayını (in Turkish).

Bakır T (2017). Tracing the Persians' footsteps in Anatolia. In: İren K, Karaöz Ç, Kasar Ö (editors). The Persians: Power and Glory in Anatolia. İstanbul, Turkey: Yapı Kredi Yayınları, pp. 2-9.

Baltacıoğlu H (2005). Arinna kentinin suları, su yapıları ve Alacahöyük. Archivium Anatolicum 8: 1-46 (in Turkish).

Barka AA (1997). Neotectonics of the Marmara Region: In: Schindler C, Pfister M (editors). Active Tectonics of Northwestern Anatolia-The Marmara Poly-Project. Zurich, Switzerland: Hochschul-verlag AG an der ETH, pp. 55-87.

Bulut H (2017). Earthly paradises: Persian gardens and paradeisoi. In: In: İren K, Karaöz Ç, Kasar Ö (editors). The Persians: Power and Glory in Anatolia. İstanbul, Turkey: Yapı Kredi Yayınları, pp. 74-183.

Çağatay MN, Eriş K, Ryan WBF, Sancar Ü, Polonia A et al. (2009). Late Pleistocene-Holocene evolution of the northern shelf of the Sea of Marmara. Marine Geology 265: 87-100.

Çağatay MN, Görür N, Algan O, Eastoe C, Tchapalyga A et al. (2000). Last glacial-Holocene palaeoceanography of the Sea of Marmara: timing of last connections with the Mediterranean and the Black Seas. Marine Geology 167 : 191-206.

Çağatay MN, Görür N, Flecker R, Sakınç M, Tünoğlu T et al. (2006). Paratethyan - Mediterranean connectivity in the Sea of Marmara region (NW Turkey) during the Messinian. Sedimentary Geology 188-189: 171-188.

Çağatay MN, Görür N, Polonia A, Demirbağ E, Sakınç M et al. (2003). Sea level changes and depositional environments in the İzmit Gulf, eastern Marmara Sea, during the late glacial-Holocene period. Marine Geology 202: 159-173.

Chaput E (1936). Voyages d'études géologiques et géomorphogéniques en Turquie. Paris, France: Mémoires de l'Institut français d'archéologie de Stamboul (in French).

Dean WE (1999). The carbon cycle and biogeochemical dynamics in lake sediments. Journal of Paleolimnology 21: 375-393.

Dereboylu E (2003). Daskyleion kabartmalı kaseleri ve batı yamacı kapları. Kronoloji ve üretim problemleri. In: Abadi-Reynal C (editor). Les céramiques en Anatolie aux époques hellénistique et romaine. Actes de la Table ronde d'Istanbul. Paris, Franch: Varia Anatolica, pp. 55-63 (in Turkish).

DSİ (1980). Aşağı Susurluk Havzası Hidrojeolojik Etüd Raporu. Ankara, Turkey: Devlet Su İşleri Genel Müdürlüğü (in Turkish).

Dypvik H, Harris NB (2001). Geochemical facies analysis of fine-grained siliciclastics using Th/U, Zr/Rb and (Zr + Rb)/Sr ratios. Chemical Geology 181: 131-146.

Eastwood WJ, Roberts C, Lamb HF, Tibby JC (1999). Holocene environmental change in southwest Turkey; a palaeoecological record of lake and catchment-related changes. Quaternary Science Reviews 18: 671-695.

Emre Ö, Duman TY, Özalp S, Elmacı H, Olgun Ş et al. (editors) (2013). Açıklamalı Türkiye Diri Fay Haritası. Ankara, Turkey: General Directorate of Mineral Research and Exploration Special Publication Series (in Turkish).

Emre Ö, Erkal T, Tchapalyga A, Kazancı N, Keçer M et al. (1998). Neogene-Quaternary evolution of the eastern Marmara region, Northwest Turkey. Bulletin of Mineral Research and Exploration 120: 119-145.

Emre Ö, Kazancı N, Erkal T, Karabıyıkoğlu M, Kuşçu İ (1997). Uluabat ve Manyas göllerinin oluşumu ve yerleşim tarihçesi. In: Kazancı N, Görür N (editors). İç Güney Marmara Bölgesi'nin Neojen ve Kuvaterner Evrimi. YDABCAG-426/G. Ankara, Turkey, TÜBİTAK, pp. 116-134 (in Turkish).

Erentöz C (1956). Türkiye jeolojisi üzerine genel bir bakış. Maden Tetkik ve Arama Dergisi 48: 37-52 (in Turkish).

Ergun Z (2013). Investigation of organic matter content of Late Quaternary sediments in Lake Manyas and surrounding area, Balıkesir, NW Turkey. MSc, Ankara University, Ankara, Turkey (in Turkish with an English abstract).

Erinç S (1956). Yalova civarında bahri Pleyistosen depoları ve taraçaları. Türk Coğrafya Dergisi 15-16: 188-190 (in Turkish).

Erinç S (1957). Karacabey Boğazı. İstanbul Üniversitesi Coğrafya Enstitüsü Dergisi 4: 95-97 (in Turkish).

Eriş K, Çağatay MN, Akçer S, Gasperini G, Mart M (2010). Late glacial to Holocene sea-level changes in the Sea of Marmara: new evidence from high-resolution seismics and core studies. Geo-Marine Letters 31: 1-18.

Eriş K, Ryan WBF, Çağatay MN, Sancar U, Lericolais G et al. (2007). Timing and evolution of the post-glacial transgression across the Sea of Marmara shelf south of Istanbul. Marine Geology 243: 57-76.

Erkmen B, Yerli SV, Erk Akan F, Kolankaya D (2013). Persistent organochlorine pesticide residues in water and sediment samples from Lake Manyas, Turkey. Journal of Environmental Biology 34: 171-176.

Erol O (1968). Çanakkale Boğazı çevresinin jeomorfolojisi hakkında ön not. Coğrafya Araştırmaları Dergisi 2: 53-71 (in Turkish).

Erol O (1981). Neotectonic and geomorphic evolution of Turkey. Zeitschrift für Geomorphologie N.F. Suppl. Bd. 40: 193-211.

Erol O (1982). Batı Anadolu genç tektoniğinin jeomorfolojik sonuçları. In: Türkiye Jeoloji Kurultayı Batı Anadolu'nun Tektoniği ve Volkanizması Paneli. Ankara, Turkey: Türkiye Jeoloji Kurumu Yayını, pp. 15-21 (in Turkish).

Erol O (1991). 1/1000 000 Scale Geomorphological Map of Turkey. Ankara, Turkey: General Directorate of Mineral Research and Exploration.

Evliya Çelebi (1648). Seyahatmane (Yayına Hazırlayan; Seyit Ali Kahraman, 2013). İstanbul, Turkey: Yapı Kredi Yayınları (in Turkish).

Görür N, Çağatay MN, Sakınç M, Sümengen M, Şentürk K et al. (1997). Origin of the Sea of Marmara from Neogene to Quaternary paleogeographic Evolution of its frame. International Geology Reviews 39: 342-352.

Gürer ÖF, Sangu E, Özburan M (2006). Neotectonics of the SW Marmara Region, NW Anatolia, Turkey. Geological Magazine 143: 1-13.

Gürer ÖF, Sangu E, Özburan M, Gürbüz A, Gürer A (2016). Plio-Quaternary kinematic development and paleostress pattern of the Edremit basin, western Turkey. Tectonophysics 679: 199-210.

Haberzetti T, Corbella H, Fey M, Janssen S, Lücke A et al. (2007). Lateglacial and Holocene Wet-dry cycles in southern Patagonia: chronology, sedimentology and geochemistry of a lacustrine record from Laguna Potrok Aike, Argentina. The Holocene 17: 297-310.

Halaçoğlu A (1995). Balkan Savaşları sırasında Rumeli'den Türk Göçleri. Ankara, Turkey: Türk Tarih Kurumu Basımevi (in Turkish).

Harrison TP (2013). Landscapes of power: neo-Hittite citadels in comparative perspective. In: Redford S, Ergin N (editors). Cities and Citadels in Turkey; From the Iron Age to the Seljuks. Leuven, Belgium: Peeters Publishing, pp. 97-114.

Helvacı C (1984). Occurrence of rare borate minerals: veatchite-A, tunnellite, terrugite and cahnite in the Emet borate deposits, Turkey. Mineral Deposita 19: 217-226.

Helvacı C, Orti F (1998). Sedimentology and diagenesis of Miocene colemanite-ulexite deposits (western Anatolia, Turkey). Journal of Sedimentary Research 68: 1021-1033.

Hume JCC, Lyons EJ, Day KP (2003). Malaria in antiquity; a genetics perspective. World Archaeology 35: 180-192.

İren K (2012). Daskyleum: The multicultural society of a Persian satrapy capital. Current World of Archaeology 54: 49-51.

İren K (2013). Daskyleion. In: Bagnall RS, Brodersen K, Champion CB, Erskine A, Huebner SR (editors). The Encyclopedia of Ancient History. Oxford, UK: Wiley-Blackwell, pp. 1930-1931.

İren K, Kazancı N, Ergun Z, Gürbüz A, Koç K, Yedek Ö et al. (2012). Manyas Gölü'nün Evrimi ve Beraberindeki Daskyleion Üzerindeki Etkileri. Proje 109K363. Ankara, Turkey: TÜBİTAK (in Turkish).

İren K, Yıldızhan H (2017). Persian Dascyleum; a Satrapal Center in the Southern Marmara Region. In: İren K, Karaöz Ç, Kasar Ö (editors). The Persians: Power and Glory in Anatolia. İstanbul, Turkey: Yapı Kredi Yayınları, pp. 332-345.

Jones B, Manning DAC (1994). Comparison of geochemical indices used for the interpretation of paleoredox conditions in ancient mudstones. Chemical Geology 111: 111-129.

Kaplanoğlu R (1999). Bursa'da Mübadele; 1923-1930 Yunanistan Göçmenleri. İstanbul, Turkey: Avrasya Etnografya Vakfı Yayınları (in Turkish).

Kazancı N, Bayhan E, Suliman N, Şahbaz A, İleri Ö et al. (1997). Manyas Gölü ve Güncel tortulları. In: Kazancı N, Görür N (editors). Güney Marmara Bölgesinin Neojen ve Kuvaterner Evrimi. YDABCAG-426/G. Ankara, Turkey: TÜBİTAK, pp. 192-238 (in Turkish).

Kazancı N, Emre Ö, Erkal T, Ileri Ö, Ergin M et al. (1999). Morphology and sedimentary facies of modern Kocasu and Gönen rivers deltas, northwestern Anatolia. Mineral Research and Exploration Bulletin 121: 1-18 (in Turkish and English).

Kazancı N, Emre Ö, Erturaç K, Leroy SAG, Öncel S et al. (2014). Possible incision time of the large valleys in southern Marmara region, Turkey. Bulletin of the Mineral Research and Exploration 148: 1-17.

Kazancı N, Görür N (1997). Güney Marmara Bölgesinin Neojen ve Kuvaterner Evrimi. YDABCAG-426/G. Ankara, Turkey: TÜBİTAK (in Turkish).

Kazancı N, Ileri O, Suliman N, Özdoğan M, Bayhan E et al. (1998). Ulubat Gölü'nde güncel tortullaşma. In: Marmara Denizi Güneyi Kıyı ve Kıyı Ardı Istiflerinin Stratigrafisi, Sedimantolojisi ve Morfotektonigi. TÜBİTAK Raporu, YDABCAG - 598/G. Ankara, Turkey: TÜBİTAK, pp. 99-145 (in Turkish).

Kazancı N, Leroy SAG, Ileri O, Emre O, Kibar M et al. (2004). Late Holocene erosion in NW Anatolia from sediments of Lake Manyas, Lake Ulubat and the southern shelf of the Marmara Sea, Turkey. Catena 57: 277-308.

Kazancı N, Öncel S, Leroy SAG, İleri Ö, Costa P et al. (2010). Wind effect on deposition of metal ions in a shallow fresh water lacustrine system: heavy metal content of Lake Ulubat sediment, NW Anatolia, Turkey. Journal of Paleolimnology 43: 89-110.

Kazancı N, Toprak Ö, Leroy SAG, Öncel S, İleri Ö et al. (2006). Boron content of Lake Ulubat sediment: a key to interpret the morphological history of NW Anatolia, Turkey. Applied Geochemistry 21: 234-251.

Kürçer A, Özaksoy V, Özalp S, Güldoğan ÇU, Özdemir E et al. (2017). The Manyas fault zone (southern Marmara region, NW Turkey): active tectonics and paleoseismology. Geodinamica Acta 29: 42-61.

Kuzucuoğlu C, Dörfler W, Kunesch S, Goupille F (2011). Mid- to late-Holocene climate change in central Turkey: the Tecer Lake record. The Holocene 21: 173-188.

Lemcke G, Sturm M (1997). $d^{18}O$ and trace element measurements as proxy for the reconstruction of climatic changes at Lake Van (Turkey). In: Dalfes HN, Kukla G, Weiss H (editors). Third Millennium BC Climate Change and Old World Collapse. Berlin, Germany: Springer, pp. 653-678.

Le Mort F, Chataigner C, Basak AN, Özbal H, Özbek M et al. (2006). From bone change to DNA: the hereditary anaemias in ancient populations of the Near East. *In*: Battini L, Villard P (editors). *Médecine et Médecins au Proche Orient Ancien,* Actes du colloque international organisé à Lyon, 8–9 November 2002. Oxford, UK: Archaeopress (BAR International Series 1528), pp. 91-101.

Leroy SAG, Kazancı N, İleri Ö, Kibar M, Emre Ö et al. (2002). Abrupt environmental changes within a late Holocene lacustrine sequence south of the Marmara Sea (Lake Manyas, N-W Turkey): possible links with seismic events. Marine Geology 190: 531-552.

Mayewski PA, Rohling EE, Stager JC, Karlen W, Maasch KA et al. (2004). Holocene climate variability. Quaternary Research 62: 243-255.

Meriç E, Nazik A, Avşar N, Alpar B, Ünlü S et al. (2009). Kuvaterner'de olası Marmara Denizi-İznik Gölü bağlantısının delilleri: İznik gölü (Bursa-KB Türkiye); Güncel sedimanlarindaki ostrakod ve foraminiferlerin değerlendirilmesi. İstanbul Yerbilimleri Dergisi 22: 1-19 (in Turkish).

Meyers PA, Lallier V (1999). Lacustrine sediment organic matter records of Quaternary paleoclimates. Journal of Paleolimnology 21: 345-372.

Miebach A, Niestrath P, Roeser P, Litt T (2016). Impacts of climate and humans on the vegetation in northwestern Turkey: palynological insights from Lake Iznik since the Last Glacial. Climate Past 12: 575-593.

MTA (2002). İstanbul and İzmir Sheets at Scale of 1/500,000. Geological Maps of Turkey. Ankara, Turkey: General Directorate of Mineral Research and Exploration of Turkey.

Nazik A, Meriç E, Avşar N, Gökaşan E (2011). Possible waterways between the Marmara Sea and the Black Sea in late Quaternary; evidence from ostracod and foreminifer assemblages in lakes İznik and Sapanca, Turkey. Geo-Marine Letters 31: 75-86.

Özbek O (2012). Sea level changes and prehistoric sites on the coasts of Southern Turkish Thrace, 12,000-6000 BP. Quaternary International 261: 162-175.

Özcan KE (2016). Soğuk savaş döneminde Bulgaristan Türklerinin Türkiye'ye göçü. MA, Hacettepe University, Ankara, Turkey (in Turkish).

Öziş Ü (2015). Water works through four millennia in Turkey. Environmental Processes 2: 559-573.

Philippson A (1915). Reisen und Forschungen im westlichen Kleinasien, Petermanns Mitt. Erdk. 2. Berlin, H.183. Gotha, Germany: Julius Perthes (in German).

Reineck HE, Singh IB (1980). Depositional Sedimentary Environments (2nd Ed.). Berlin, Germany: Springer Verlag.

Roberts N, Eastwood WJ, Kuzucuoğlu C, Fiorentino G, Caracuta V (2011). Climatic, vegetation and cultural change in the eastern Mediterranean during the mid-Holocene environmental transition. The Holocene 21: 147-162.

Roberts N, Reed JM, Leng MJ, Kuzucuoğlu C, Fontugne M et al. (2001). The tempo of Holocene climatic change in the eastern Mediterranean region: new high resolution crater-lake sediment data from central Turkey. The Holocene 11: 721-736.

Roeser PA, Franz SO, Litt T, Ülgen UB, Hilgers A et al. (2012). Lithostratigraphic and geochronological framework for the paleoenvironmental reconstruction of the last ~36 ka cal BP from a sediment record from Lake Iznik (NW Turkey). Quaternary International 274: 73-87.

Ryan WBF, Pitman WC, Major CO, Shimkus K, Moskalenko V et al. (1997). An abrupt drowning of the Black Sea shelf. Marine Geology 138: 119-126.

Sakınç M, Bargu S (1989). İzmit Körfezi güneyindeki geç Pleyistosen (Tireniyen) çökel stratigrafisi ve bölgenin neotektonik özellikleri. Türkiye Jeoloji Bülteni 32: 52-64 (in Turkish).

Sakınç M, Yaltırak C (1997). Güney Trakya sahillerinin denizel Pleyistosen çökelleri ve paleocoğrafyasi. Bulletin of Mineral Research and Exploration 119: 43-62 (in Turkish).

Şaroğlu F, Emre Ö, Boray A (1987). Türkiye'nin Diri Fayları ve Depremsellikleri. Maden Tetkik ve Arama Genel Müdürlüğü Rapor No: 8174. Ankara, Turkey: MTA (in Turkish).

Smith NE (2015). The Paleoepidemiology of Malaria in the Ancient Near East. PhD, University of Arkansas, Fayetteville, AR, USA.

TÜİK (2016). Family Structure Survey Micro Dataset. Turkish Statistic Institute, Publication No. 4475. Ankara, Turkey: Türkiye İstatistik Kurumu.

Ülgen UB, Franz SO, Biltekin D, Çagatay MN, Roeser PA et al. (2012). Climatic and environmental evolution of Lake Iznik (NW Turkey) over the last 4700 years. Quaternary International 274: 88-101.

Vita-Finzi C (1969). Late Quaternary continental deposits of central and western Turkey. Man 4: 605-619.

Yaltırak C, Ülgen UB, Zabci C, Franz SO, Ön SA et al. (2012). Discussion: A critique of Possible waterways between the Marmara Sea and the Black Sea in the late Quaternary: evidence from ostracod and foraminifer assemblages in lakes İznik and Sapanca, Turkey, Geo-Marine Letters, 2011. Geo-Marine Letters 32: 267-274.

Appendix 1. Major element compositions of SK3 samples.

Depth (m)	Major elements (%)													
	Na_2O	MgO	Al_2O_3	SiO_2	P_2O_5	SO_3	K_2O	CaO	TiO_2	V_2O_5	Cr_2O_3	MnO	Fe_2O_3	LOI
0.35	0.38	2.65	13.69	62.08	0.94	0.41	2.96	5.97	0.62	0.02	0.03	0.14	5.13	4.38
0.55	0.21	2.63	13.32	62.69	0.33	0.32	2.78	7.69	0.56	0.02	0.03	0.13	4.80	3.76
0.7	0.41	2.78	13.09	61.13	0.43	0.31	2.80	5.38	0.58	0.01	0.01	0.12	4.68	7.33
0.9	0.20	3.00	13.36	59.90	0.60	0.31	2.86	8.21	0.61	0.02	0.03	0.15	5.03	4.76
1.25	0.59	2.57	12.57	57.25	0.72	0.67	2.68	10.08	0.55	0.02	0.02	0.09	4.43	7.37
1.55	0.25	2.29	10.96	54.14	0.42	0.25	2.73	13.32	0.46	0.02	0.05	0.09	4.67	10.73
1.65	0.16	2.39	11.61	59.12	0.41	0.29	2.87	11.27	0.47	0.02	0.03	0.07	3.60	6.33
1.85	0.20	2.97	12.47	52.29	0.27	0.21	2.89	12.22	0.54	0.01	0.01	0.08	4.30	10.23
2.0	0.08	2.84	12.36	48.43	0.70	0.64	2.80	15.00	0.56	0.02	0.01	0.10	4.79	10.87
2.25	0.08	2.85	12.18	48.12	0.72	0.24	2.65	16.26	0.54	0.02	0.02	0.09	4.50	10.89
2.45	0.08	2.92	11.94	49.11	0.91	0.63	2.66	13.33	0.55	0.02	0.02	0.09	4.57	12.73
2.65	0.08	2.74	11.13	45.37	0.35	0.62	2.94	17.83	0.52	0.02	0.02	0.10	4.33	13.28
2.85	0.07	0.83	2.93	12.37	0.12	0.13	0.62	47.83	0.16	0.00	0.00	0.06	1.23	33.82
3.05	0.09	3.04	13.12	54.98	0.61	0.22	2.84	10.14	0.59	0.02	0.01	0.11	4.99	7.93
3.25	0.14	2.87	13.11	57.22	0.84	0.25	2.71	11.01	0.59	0.02	0.03	0.08	4.92	5.37
3.45	0.09	2.90	12.78	58.25	0.49	0.24	2.86	11.46	0.55	0.02	0.04	0.08	4.47	4.98
3.65	0.46	2.88	17.70	63.68	0.14	0.25	3.07	1.60	0.73	0.02	0.03	0.05	5.64	3.28
3.8	0.09	2.82	13.36	57.11	0.63	0.27	2.81	11.04	0.61	0.02	0.01	0.06	4.86	5.38
4.0	0.08	2.85	12.24	50.72	0.54	0.23	2.66	13.42	0.59	0.02	0.02	0.08	4.80	10.33
4.2	0.16	3.18	13.07	54.46	0.44	0.21	2.71	11.79	0.59	0.02	0.02	0.07	4.49	7.93
4.4	0.09	3.10	12.58	53.06	0.51	0.24	2.79	12.97	0.59	0.02	0.01	0.11	4.87	7.83
4.6	0.08	2.74	11.23	45.34	0.31	0.19	2.34	19.10	0.54	0.01	0.02	0.09	3.94	12.92
4.8	0.12	3.78	14.11	56.71	0.36	0.33	2.36	13.26	0.43	0.01	0.01	0.06	3.27	5.28
5.05	0.09	3.10	12.57	50.99	0.41	0.23	2.61	19.96	0.61	0.02	0.01	0.11	4.69	3.72
5.2	0.09	3.02	13.68	53.11	0.90	0.23	2.98	14.68	0.60	0.02	0.03	0.12	5.19	4.87
5.4	0.09	2.69	11.70	51.11	0.97	0.21	2.39	15.20	0.59	0.01	0.01	0.08	3.96	10.38
5.6	0.47	2.76	10.65	52.74	0.82	0.18	2.18	15.15	0.64	0.02	0.05	0.07	3.67	10.77
5.8	0.54	1.27	7.69	47.61	0.19	0.15	1.54	22.12	0.44	0.01	0.01	0.04	2.40	16.39
6.0	0.08	2.86	12.35	51.56	0.72	0.72	2.62	13.84	0.57	0.01	0.01	0.08	4.34	10.76
6.2	0.08	1.49	7.81	30.71	0.09	0.14	1.82	24.84	0.43	0.02	0.03	0.04	3.14	28.37
6.4	1.91	1.92	11.85	66.97	0.19	0.18	2.65	8.01	0.55	0.02	0.01	0.03	3.04	2.47
6.6	0.09	2.71	11.54	52.07	0.30	0.19	2.61	15.25	0.60	0.01	0.01	0.08	4.26	10.33
6.8	0.25	2.43	11.52	57.12	0.34	0.22	2.34	16.55	0.84	0.03	0.08	0.08	4.58	2.81
7.05	0.50	2.88	13.05	57.40	0.15	0.17	3.33	12.56	0.58	0.02	0.01	0.04	3.93	6.37
7.2	0.36	4.30	15.63	56.64	0.07	0.21	3.85	3.70	0.61	0.02	0.02	0.06	5.80	7.98
7.4	1.24	3.83	16.86	64.10	0.11	0.21	4.21	1.26	0.63	0.02	0.01	0.04	4.87	2.37
7.6	0.84	3.44	16.58	55.76	0.12	0.20	4.29	8.71	0.68	0.02	0.05	0.06	5.33	3.28
7.8	0.74	3.94	16.63	57.94	0.10	0.21	4.63	4.70	0.75	0.02	0.02	0.07	5.52	3.98
8.0	0.33	3.41	15.30	52.10	0.10	0.19	4.04	13.87	0.66	0.02	0.03	0.18	5.27	5.33
8.2	0.66	3.98	17.03	60.89	0.13	0.18	4.53	1.41	0.69	0.02	0.01	0.04	5.39	4.38
8.4	0.63	4.28	17.81	55.49	0.12	0.19	4.75	6.86	0.70	0.02	0.02	0.08	5.43	3.03
8.6	0.64	4.23	17.57	59.27	0.08	0.20	4.81	2.15	0.72	0.03	0.02	0.04	5.97	3.67
8.8	1.15	3.47	16.19	62.19	0.12	0.21	4.01	2.71	0.59	0.02	0.06	0.04	4.68	3.87
9.0	0.26	2.64	12.60	50.63	0.13	0.18	3.25	19.11	0.54	0.01	0.01	0.17	4.36	6.78
9.2	0.24	3.05	13.57	56.48	0.66	0.23	2.92	10.78	0.62	0.02	0.01	0.09	4.97	7.26
9.4	1.69	2.93	14.24	64.20	0.16	0.19	3.44	4.04	0.53	0.01	0.01	0.04	3.90	4.27
9.6	1.28	2.87	13.23	61.02	0.11	0.20	3.13	7.60	0.56	0.03	0.08	0.05	3.82	6.66
9.8	0.23	3.55	14.35	54.01	0.14	0.20	3.23	11.20	0.66	0.03	0.01	0.06	6.78	4.76
10.0	0.17	3.41	13.71	48.44	0.14	0.17	2.92	10.47	0.60	0.03	0.02	0.05	7.83	11.37

Appendix 2. Trace element compositions of SK-3 samples.

Depth (m)	Trace Elements (ppm)																														
	Co	Ni	Cu	Zn	Ga	Ge	As	Se	Br	Rb	Sr	Y	Zr	Nb	Mo	Cd	Sn	Sb	Te	I	Cs	Ba	La	Ce	Hf	W	Hg	Tl	Pb	Bi	Th	U
0.35	28.4	30.2	26.4	67.1	13.3	1.9	12.8	0.4	5.9	121	243.1	19.2	208.1	10.3	4.7	0.8	1.4	2.1	1.2	4.3	16.6	849	33.4	54.2	5.7	16	1.4	1.1	45.4	1	15.6	7
0.55	20	31.7	22.9	57.5	13.8	1.6	16.8	0.5	5.6	115.7	245	16.5	160.1	6.9	2.9	0.8	2.2	2.1	1.3	5.5	18.5	889.6	42.4	69.9	6.4	30	1.5	1.9	46.5	1	15.7	6.9
0.7	22.6	31.8	24.9	62.7	15.6	1	18	0.5	8.2	120.5	285.5	19.2	180.4	10.6	2.5	0.8	2.2	1	1.3	3.4	17.1	856.3	33.7	54.7	4.9	20.4	1.3	0.8	43.5	1	13.8	6.9
0.9	33.1	31.9	28.9	72	15	0.8	18.7	0.5	7.2	125.8	299.9	19.3	160.7	10	6.4	0.8	1.5	2.7	1.3	4.5	18.6	856.9	34.9	63.6	4.5	26.4	1.4	1.7	46.7	0.6	15.3	8
1.25	27.8	31.7	28.5	71.7	15.7	1.4	18.5	0.5	6.1	116.7	333	19.1	141.7	12.3	2.2	0.8	2.1	0.7	1.3	2.4	16.5	847.5	29	51.9	4.7	36.6	1.6	1.4	40.7	1	13.8	7.4
1.55	35.6	28.7	19.1	47.1	13.2	1	11.1	0.5	5.1	109.4	309.1	17.7	143.1	9.8	3.2	0.9	1.6	0.5	0.9	3	16.3	719.8	32.3	53.6	6.6	45.3	1.6	1.3	34.1	0.4	11.4	8.4
1.65	17	27.6	17	41	10.4	1.1	9.5	0.4	6.8	107.5	273.1	16.5	159	7.3	3.1	0.9	6.8	1.7	1.4	2.5	13.2	748.3	25.3	46.3	5.7	22.3	1.4	0.7	33.9	1	10	7.8
1.85	28.8	32.3	18.2	47.6	16.4	0.9	13.3	0.5	3.1	155.5	249.1	18.3	172.1	12.9	3.2	0.9	2.8	1.9	1.3	2.4	22.9	716.3	26.3	51.2	3.7	35.3	1.5	0.8	26.7	0.5	13.7	9.4
2	21	40.5	21.4	51.1	16.5	1.6	11.3	0.4	3.6	152.1	242.5	16.8	166.9	17.6	5.5	7.4	12.4	9.6	1.7	2.8	34.9	890.2	39.7	60.4	5.9	15.7	1.4	1.6	30.4	1.1	14.8	20.6
2.25	22.6	37.3	25.5	50.4	16.7	1.9	9.7	0.4	3.3	141	272.3	19.4	167.3	13.1	4.7	0.9	1.9	1.8	1.4	4.8	23.4	873.5	39.5	61	3.9	13	1.5	1.5	35.9	0.6	13.2	9
2.45	19.7	34.5	23.1	54.9	15.9	1.9	26.8	0.5	3.5	140.1	317.1	19.6	161.7	7.7	5.7	0.9	1.9	1.3	1.3	6.2	21	880	61.3	90.9	5.3	15.6	1.5	0.8	35	1.1	15.6	9.7
2.65	26.9	34	24.5	51.5	14.7	1.2	11.1	0.5	3.1	131.5	285.7	16.5	134.1	12.9	3	0.5	2.5	1.1	1.4	5.4	20.1	791.9	26.8	46.1	5.3	16.2	0.9	1.5	37.5	1.1	15.5	8.7
2.85	20	9	4.1	14.6	5.4	0.8	4.4	0.5	1.6	41.2	410.7	4.5	41.5	4.1	3.5	1	0.5	1.1	1.4	5.6	3.9	246.9	16.8	14.4	4.8	3.6	1.5	1.5	13.1	1.1	5.6	9.2
3.05	22.4	38.5	29.6	67.5	16.3	1.3	12.2	0.4	3.1	147.1	248.7	20.1	159.2	11.3	2.9	0.8	3.3	0.8	1.3	5.1	33.1	859.3	47.2	75.8	4.8	11.1	1.4	1.6	33.3	1	15.5	6.3
3.25	21	34.3	29.4	73.5	15.8	1.3	13.2	0.5	6.5	134.2	286.6	21.3	180.4	11.2	3.1	0.9	2.2	0.9	1.3	4	22.2	877.7	35.7	59.9	5.4	34.5	1.6	1.3	34.5	1.1	13.9	7.7
3.45	24	33.8	21.9	55.1	15.1	1.9	10.1	0.5	3.4	143.2	216.8	22.4	181.2	9.7	3.3	0.9	2.6	1.5	1.4	2.6	27.1	804.8	29.9	59.3	4.4	34.8	1.5	1.4	27.9	1	14	8.1
3.65	21.7	49.4	18.6	57.1	19.8	1.5	26.4	0.4	2.7	124.7	141.8	32.5	229.8	14.2	4.3	0.8	2.7	1.3	1.3	2.3	13.1	664.9	44.3	79.1	4.3	32.6	1.5	0.6	22.6	0.7	11.3	7
3.8	21	33	28.3	63.9	16	1.7	13.8	0.5	5	131.1	293.8	19.8	157.3	14.4	3.2	0.9	2.7	2.2	1.3	2.5	15.2	848.8	33	57.4	5.9	28	1.5	1.5	35	0.9	15.8	8.2
4	19.8	36.4	29	61.2	16.2	2.1	12.1	0.4	3.7	134.5	271.5	17.2	155.5	13.2	3.1	0.9	2.6	1.5	1.3	4.9	15.5	885.9	39	64.1	6.1	7	1.4	1.4	40	1.1	15.8	7
4.2	22.5	31.8	25.2	54.4	16.9	1.2	13.5	0.5	3.4	139.9	256	18	166.7	12.3	3.3	0.8	3.2	3.2	1.3	2.5	16.6	837.3	23.5	47.3	4.7	23.2	1.5	1.5	40	1.1	17.5	7.6
4.4	22.1	38	26.8	60.2	15.7	1.1	12.7	0.5	3.5	134.8	262	16.5	169.8	16.3	7.8	1	2.1	2.6	1.4	2.6	20.1	899.1	28.7	58.7	8.2	14.7	1.4	0.9	36.6	0.5	14.8	8.8
4.6	20	33.6	23.5	43.8	14.4	2.3	11.7	0.5	3.2	122.3	280.3	16.6	141.2	16.3	3.5	0.8	2.6	1	1.3	3.6	9.6	673	29.2	60.7	4.6	10.8	1.5	1.9	36	0.7	17.5	11.9
4.8	18	21.4	18.1	42.1	12.5	1.4	8.2	0.4	3.6	100.9	223.8	13.8	95.5	7	3.7	0.9	0.8	1.2	1.6	5.3	12.1	464.6	22.6	28	3.8	7.1	1.2	0.9	26.3	0.9	14.1	7.9
5.05	29	30.6	25.3	48.7	14.4	1.4	11.2	0.5	3.4	125.2	286.3	14.9	139.9	12.8	3.5	0.6	3.5	4	0.6	3.4	12.2	815.7	20.7	43.2	4.7	14	1.4	0.8	36.4	1.1	17.3	13.4
5.2	29.2	39.7	21.9	50.9	16.2	1.9	13.9	0.5	2.3	156	243.8	18	164.7	13.9	4.4	0.7	1.8	2.3	1.2	10.5	24.4	823.3	30.2	50.3	4.5	12.6	1.5	1.3	28.1	0.8	12.7	7.1
5.4	22.2	26.7	16.8	45.5	14	1	12.2	0.5	1.9	127.8	234.8	22.6	201.9	12.3	3.2	0.8	3.1	1	1.3	5.8	24.2	662.5	31	49.4	4.3	46.2	1.6	1.4	29.1	1.1	13.2	7.7
5.6	21.4	22.8	5	31.6	13.1	2.2	7.3	0.5	1.6	129.7	167.8	28	199.6	15	4.7	0.7	3.8	1.4	1.3	2.3	21.1	394.4	23.3	51	6	40.6	1.6	0.9	17.3	0.9	7.1	7.8
5.8	16	14.4	2.5	21.2	9.4	1.1	6.4	0.5	0.9	98.8	164.6	24.9	152.2	5.9	3.6	0.9	1.4	1	2.1	2.2	18	260.4	17.6	37.4	4.1	53.3	1.7	1.3	14	0.9	9.6	8.9
6	25.3	31.9	24.5	53.1	14.4	1.2	10.5	0.5	2.7	139.1	237.6	18	168.5	11.2	3.1	0.9	2	1.4	1.3	5	23.2	755.2	27.3	40.5	4.6	24.4	1.5	0.7	32.8	1	14.7	8.2
6.2	19	24.6	9.1	32.4	13.6	0.5	6.5	0.5	0.8	165.5	176.3	23.6	178.4	8.6	4.1	0.8	2.2	0.8	1.3	2.6	31.7	356.8	31.4	50.5	4.7	23.8	1.6	1.5	14.7	0.5	7.2	7.4
6.4	30.4	22.3	16.3	36.7	14.7	0.9	7.5	0.6	0.5	162.8	153.2	23.2	225	14	3.8	0.4	3.8	1	1.2	2.2	31	356	23.9	43	3.7	135.3	2.1	1.3	16.4	0.9	6.4	11.4
6.6	19	29.3	16.2	41.5	13.4	1	9.3	0.5	1.5	134.8	200.6	22.9	193.7	12	2.8	0.8	1.2	10.6	1.3	2.4	24.6	550.3	31.8	70.5	4	34.8	1.5	1.4	22.1	0.9	10.7	8.1
6.8	19.7	26.3	14.6	34.2	12.1	1.5	14.8	0.5	1.8	106.3	186.5	28.9	281.6	13.9	3.5	0.8	1.6	1.1	1.4	2.4	24.3	441	29.8	58.3	6	50	1.6	1.3	19	1	9	7.3
7.05	21.6	24	7.7	38.1	14.8	1.4	9.7	0.4	0.7	220	148.1	17.8	140.9	10.2	5.5	0.8	3	0.9	1.3	2.2	49.9	456.4	21.8	36.6	3.5	32.8	1.5	0.6	15.9	0.9	6.3	7.8
7.2	24.8	53.6	26.3	66.8	20.4	2.9	5.4	0.5	0.5	268.3	189.8	21.4	176.6	19.4	8	7.6	12.7	1.3	1.5	12.6	63	620.5	46.2	74.2	5.7	10.4	1.5	1.8	26.7	1	15.9	20.7
7.4	23.5	40.2	14.9	57.7	22.5	2.1	5.9	0.5	0.4	232.2	153.5	22.1	224.1	16.8	6.4	6.7	13.1	1.2	1.5	10.4	61.8	574	38.3	67.7	4.1	76.2	1.9	0.9	16.9	0.9	12.3	24.9
7.6	27.9	31	10.3	53.5	22.7	1.5	7.8	0.4	0.5	276.8	152.6	18.6	154	16.5	3.9	0.8	6.5	1	1.3	2.3	47.9	595	19.8	33.8	7.8	24.4	1.5	1.5	13.9	0.9	7	7.5
7.8	19.2	30.9	9	59.4	23.1	1.7	7.6	0.4	0.8	299.6	147.7	17.3	158.7	16.3	4.4	5.5	12	6.3	1.5	2.6	64.5	625.9	28.8	39.8	3.8	16.7	1.4	1.3	14.8	0.9	7.2	14.6
8	21.4	32.7	10.3	55.8	23	1.6	7.4	0.5	1.1	284.8	155.6	20.9	149.2	11.2	2.8	0.8	4.4	1	1.3	2.4	55	631	14.1	36.9	3.9	15.8	1.4	0.9	15.4	0.9	5.8	8.6
8.2	28.1	32.9	7.8	57.1	22.3	2.9	8.3	0.4	1.2	306.2	142.8	16.4	149	12.9	3.3	0.9	5.5	1	1.3	2.4	79.2	599.2	24.2	43.7	5	14.7	1.4	0.8	16.2	0.9	8.2	7.3
8.4	22	32.5	18.5	65.7	22.3	2.7	7.4	0.4	0.9	307.3	149	19	141.2	15.4	6	0.9	5.7	1	1.3	2.4	69.4	649.1	20.4	39.5	3.7	21.3	1.5	0.9	16.5	0.9	6.2	7.9
8.6	28.5	33.6	10.2	65	24.1	2.6	6.7	0.4	0.5	335.6	142.5	18.5	148.6	14	2.9	0.9	5.9	1.3	1.4	2.4	93.3	618.3	35.1	49.5	3.9	16	1.4	1.4	14.9	0.9	6	8.2
8.8	20	30.2	8.5	48.2	21.3	2.4	5.1	0.4	0.4	253.8	143.1	16.6	160.4	11.1	4.3	0.8	3.6	0.9	1.3	2.3	58.6	539.5	20.2	38.8	3.6	27.3	1.5	1.4	15.3	0.9	5.9	15.5
9	19	26.4	10	44.5	20.1	1	9	0.5	0.9	250	170.4	23.3	133.4	11.9	4.8	0.9	3.5	1.4	1.3	2.3	51	552.3	25.9	40.9	3.9	49.5	1.7	1.5	20.4	1	8.4	7.2
9.2	36.6	35	27.9	65.4	18.1	2.4	11.7	0.4	4.3	153.1	241.9	21.6	177.4	13.2	3.2	0.9	1.1	1.1	1.3	5.5	33.5	848.2	38.4	73.9	4.7	12.9	1.4	1.5	31.6	1	13.6	7.7
9.4	21.6	26.6	8.7	47.3	20.7	2.5	6.7	0.6	0.3	240.1	148.4	19.1	174	14.2	6.6	5.1	11.5	6.3	1.5	2.5	67.1	513.4	29.2	45.3	3.6	95.7	2	1	16.8	0.7	7.3	18.7
9.6	31.9	24.9	6.8	33	15.2	0.7	7.2	0.5	0.9	168.4	145.5	21.3	194	11.9	3.1	0.8	2.1	1.2	1.4	2.3	41.9	434.9	31.2	53.2	3.2	47.3	1.4	0.6	18.8	0.8	7	7.7
9.8	24.1	63.4	19.3	62.2	19.1	1.6	6.3	0.4	0.4	234.7	171.5	26.1	114.6	10.4	3.5	0.9	4	1.4	1.3	2.2	71.4	491	27.8	56.7	4.7	13	1.5	1.1	20.9	1	10.2	8.1
10	51.1	93.1	37	84.4	19.1	2.9	8.5	0.5	0.6	199.5	209	33.7	113.1	16.7	3.9	1	2.9	0.7	1.3	2.4	57.2	584	38.5	91.1	5.8	6.8	1.7	1.1	25.9	1.1	18	10.1

Supplement 1. Mineral constituents detected by XRD technique of seven cores' samples. Their relative abundance is in descending order from left to right.

Core no.	Sample depth from top, m	Minerals detected
SK1	2.4	Illite, quartz, plagioclase
	14.9	Illite, quartz, plagioclase
SK2	1.0	Illite, quartz, alkali feldspar, calcite
	1.5	Illite, quartz, plagioclase, calcite
	4.2	Illite, quartz, plagioclase, calcite
	11.9	Illite, calcite, plagioclase, quartz
SK3	1.5	Illite, calcite, plagioclase, quartz
	3.4	Illite, plagioclase, quartz
	5.4	Illite, calcite, plagioclase, quartz
	7.4	Illite, plagioclase, quartz
	9.4	Illite, quartz
	11.4	Illite, calcite, plagioclase, quartz
	13.4	Illite, kaolinite, calcite, plagioclase, quartz, feldspar
SK4	4.0	Smectite, illite, calcite, plagioclase, quartz
	13.0	Feldspar, quartz
SK5	2.6	Kaolinite, illite, calcite, quartz, feldspar
	3.8	Smectite, illite, kaolinite, quartz, feldspar
	3.9	Smectite, illite, kaolinite, quartz, feldspar, calcite
	5.1	Quartz, calcite
SK6	8.2	Feldspar, quartz, calcite
SK7	1.0	Quartz, feldspar, calcite
	4.9	Illite, kaolinite, quartz, feldspar, calcite

Supplement 2. Composition of some major and trace elements of SK3's sediments used in interpretations. Compare with Figures 9 and 12.

Depth (m)	Major elements (%)			Trace elements (ppm)				
	CaO	TiO_2	LOI	Rb	Sr	Zr	Th	U
0.35	5.97	0.62	4.38	121	243.1	208.1	15.6	7
0.55	7.69	0.56	3.76	115.7	245	160.1	15.7	6.9
0.7	5.38	0.58	7.33	120.5	285.5	180.4	13.8	6.9
0.9	8.21	0.61	4.76	125.8	299.9	160.7	15.3	8
1.25	10.08	0.55	7.37	116.7	333	141.7	13.8	7.4
1.55	13.32	0.46	10.73	109.4	309.1	143.1	11.4	8.4
1.65	11.27	0.47	6.33	107.5	273.1	159	10	7.8
1.85	12.22	0.54	10.23	155.5	249.1	172.1	13.7	9.4
2.0	15.00	0.56	10.87	152.1	242.5	166.9	14.8	20.6
2.25	16.26	0.54	10.89	141	272.3	167.3	13.2	9
2.45	13.33	0.55	12.73	140.1	317.1	161.7	15.6	9.7
2.65	17.83	0.52	13.28	131.5	285.7	134.1	15.5	8.7
2.85	47.83	0.16	33.82	41.2	410.7	41.5	5.6	9.2
3.05	10.14	0.59	7.93	147.1	248.7	159.2	15.5	6.3
3.25	11.01	0.59	5.37	134.2	286.6	180.4	13.9	7.7
3.45	11.46	0.55	4.98	143.2	216.8	181.2	14	8.1
3.65	1.60	0.73	3.28	124.7	141.8	229.8	11.3	7
3.8	11.04	0.61	5.38	131.1	293.8	157.3	15.8	8.2
4.0	13.42	0.59	10.33	134.5	271.5	155.5	15.8	7
4.2	11.79	0.59	7.93	139.9	256	166.7	17.5	7.6
4.4	12.97	0.59	7.83	134.8	262	169.8	14.8	8.8
4.6	19.10	0.54	12.92	122.3	280.3	141.2	17.5	11.9
4.8	13.26	0.43	5.28	100.9	223.8	95.5	14.1	7.9
5.05	19.96	0.61	3.72	125.2	286.3	139.9	17.3	13.4
5.2	14.68	0.60	4.87	156	243.8	164.7	12.7	7.1
5.4	15.20	0.59	10.38	127.8	234.8	201.9	13.2	7.7
5.6	15.15	0.64	10.77	129.7	167.8	199.6	7.1	7.8
5.8	22.12	0.44	16.39	98.8	164.6	152.2	9.6	8.9
6.0	13.84	0.57	10.76	139.1	237.6	168.5	14.7	8.2
6.2	24.84	0.43	28.37	165.5	176.3	178.4	7.2	7.4
6.4	8.01	0.55	2.47	162.8	153.2	225	6.4	11.4
6.6	15.25	0.60	10.33	134.8	200.6	193.7	10.7	8.1
6.8	16.55	0.84	2.81	106.3	186.5	281.6	9	7.3
7.05	12.56	0.58	6.37	220	148.1	140.9	6.3	7.8
7.2	3.70	0.61	7.98	268.3	189.8	176.6	15.9	20.7
7.4	1.26	0.63	2.37	232.2	153.5	224.1	12.3	24.9
7.6	8.71	0.68	3.28	276.8	152.6	154	7	7.5
7.8	4.70	0.75	3.98	299.6	147.7	158.7	7.2	14.6
8.0	13.87	0.66	5.33	284.8	155.6	149.2	5.8	8.6
8.2	1.41	0.69	4.38	306.2	142.8	149	8.2	7.3
8.4	6.86	0.70	3.03	307.3	149	141.2	6.2	7.9
8.6	2.15	0.72	3.67	335.6	142.5	148.6	6	8.2
8.8	2.71	0.59	3.87	253.8	143.1	160.4	5.9	15.5
9.0	19.11	0.54	6.78	250	170.4	133.4	8.4	7.2
9.2	10.78	0.62	7.26	153.1	241.9	177.4	13.6	7.7
9.4	4.04	0.53	4.27	240.1	148.4	174	7.3	18.7
9.6	7.60	0.56	6.66	168.4	145.5	194	7	7.7
9.8	11.20	0.66	4.76	234.7	171.5	114.6	10.2	8.1
10.0	10.47	0.60	11.37	199.5	209	113.1	18	10.1